




ARTICLE

Disease Ecology

Landscape dynamics of a vector-borne disease in the western US: How vector–habitat relationships inform disease hotspots

Emile Elias¹  | Heather M. Savoy²  | Dustin A. Swanson³ |
Lee W. Cohnstaedt³ | Debra P. C. Peters²  | Justin D. Derner⁴ |
Angela Pelzel-McCluskey⁵ | Barbara Drolet³ | Luis Rodriguez⁶

¹US Department of Agriculture, Agricultural Research Service, Jornada Experimental Range Unit, Las Cruces, New Mexico, USA

²US Department of Agriculture, Agricultural Research Service, Big Data Initiative and the SCINet Program for Scientific Computing, Office of National Programs, Beltsville, Maryland, USA

³US Department of Agriculture, Agricultural Research Service, Arthropod-Borne Animal Diseases Research Unit, Center for Grain and Animal Health Research, Manhattan, Kansas, USA

⁴US Department of Agriculture, Agricultural Research Service, Rangeland Resources and Systems Research Unit, Cheyenne, Wyoming, USA

⁵US Department of Agriculture, Animal and Plant Health Inspection Service, Veterinary Services, Fort Collins, Colorado, USA

⁶US Department of Agriculture, Agricultural Research Service, Foreign Animal Disease Research Unit, Plum Island Animal Disease Center, Orient Point, New York, USA

Correspondence

Emile Elias

Email: emile.elias@usda.gov

Funding information

Agricultural Research Service,
Grant/Award Number:
0500-00093-001-00-D

Abstract

Vesicular stomatitis (VS) is a vector-borne viral disease that causes lesions in livestock, premises, county and state quarantines, and important economic losses. We investigated vector–habitat characteristics for vectors associated with VS in regions of recurrent disease within the western United States (US) that consistently lead to the environment where vector, host, and pathogen populations intersect to enable pathogen transmission. We analyzed the habitats of previously identified insect vectors, including black flies (BFs) (*Simulium vittatum* complex), biting midges (BMs) (*Culicoides variipennis* complex, which includes *Culicoides sonorensis*), and sand flies (SFs) (*Lutzomyia shannoni*) in six regions of interest (ROIs) containing hotspots of VS ranging from Texas (TX) to Wyoming. This analysis broadened the understanding of (1) how regions of reoccurring VS differ from the broader western US, (2) how geographically separated regions and hotspots are similar across time, and (3) how vector–environment habitat a priori knowledge relates to observed hotspots. Analysis of watershed factors (livestock densities, land-cover proportions, stream and lake densities, and irrigation methods) indicated a complex system separating areas with high, recurring VS from the broader western US. Although no single characteristic separated the six ROIs from other areas, we found two distinct emerging groups (northern ROI and TX). Hotspots, estimated from monthly VS concentrations, evolved northward throughout the year and most hotspots were closer to flowing water and agricultural land than the broader ROI. All ROIs contained environmental conditions suitable for multiple vectors at some point in the year, but BFs had the highest suitability scores, whereas BM scores were lower and varied annually with higher suitability in summer. SFs had the lowest suitability score in all ROIs, consistent with their low likelihood of being vectors. BM habitat patches were often orders of magnitude smaller than BF patches, and hotspot patches

This is an open access article under the terms of the [Creative Commons Attribution](https://creativecommons.org/licenses/by/4.0/) License, which permits use, distribution and reproduction in any medium, provided the original work is properly cited.

Published 2022. This article is a U.S. Government work and is in the public domain in the USA. *Ecosphere* published by Wiley Periodicals LLC on behalf of The Ecological Society of America.

Handling Editor: Paige Ferguson

reinforce the likelihood that BF may be the most critical vector in northern ROI, whereas both BM and BF have similar likelihood in southern ROI. Given limited existing vector data, this analysis provides an alternate pathway for using habitat information to associate likely vectors responsible for transmission. Results could support early warning and mitigation efforts to reduce the incidence of VS.

KEYWORDS

livestock, nidus, patch analysis, vector-borne disease, vesicular stomatitis virus

INTRODUCTION

Vesicular stomatitis (VS) is a vector-borne viral disease causing vesicular lesions in cattle (*Bos taurus*), equines (*Equus caballus*), and other livestock, as well as quarantines causing important economic losses due to trade interruption between countries (Peck et al., 2020). VS can present with clinical signs similar to foot-and-mouth disease, one of the most devastating livestock diseases, raising alarm and leading to challenges for livestock owners and veterinarians. We investigated vector–habitat characteristics for a suite of vectors associated with VS in regions of recurrent disease within the western United States (US) that consistently led to the nidus of pathogen transmission or the environment where vector, host, and pathogen populations intersect to enable pathogen transmission (Reisen, 2010).

VS history and occurrence

In the western US, VS outbreaks have occurred at roughly 5–10-year intervals (Rodríguez, 2002). Introductions of vesicular stomatitis virus (VSV) in the US can lead to: (1) a limited incursion event, where disease is limited to few cases in the southern US and stops after 1 year, (2) a successful incursion in one year followed by overwintering and broadscale expansion in the subsequent years, or (3) extinction years where few or no cases occur (Peters et al., 2020). Host density and VS vectors may play an important role in these patterns in VS occurrence. Recent studies have investigated the landscape and hydrologic relationships among locations supporting VS and found differing variable importance in incursion years (i.e., distance to flowing water) as compared with expansion years (i.e., soil properties) (Peters et al., 2018, 2020). Although big data approaches and spatial analyses have shed light on landscape and hydrologic relationships with VS, additional analysis at relevant spatial and temporal scales is required to infer vectors responsible for transmission, and to determine why VS incidence

consistently reappears in the same locations across different outbreak years.

Phylogenetic studies indicate that each outbreak cycle in the western US (lasting 1–3 years) is caused by a distinct viral genetic lineage originating in endemic areas in southern Mexico (Rodríguez et al., 2000). The mechanisms of incursion into the US are not fully understood, but studies suggest insect vectors rather than livestock movement are involved (Palinski et al., 2021; Rodríguez, 2002). A reservoir host for VSV leading to outbreaks in domestic livestock on the US mainland has not been confirmed; however, feral swine were believed to contribute to the establishment of a VSV-endemic cycle on Ossabaw Island off the coast of Georgia, USA (Killmaster et al., 2010). However, a similar role of feral swine in VSV transmission in the western US is currently unlikely since it is outside their current footprint. If the footprint of feral swine expands to increase co-occurrence with livestock in the western US, then there may be an increase in cross-species transmission (Miller et al., 2017), but this hypothesized host would then need to be investigated.

Insect vectors and habitats

In the US, there are three groups of demonstrated VSV insect vectors: black flies (BFs; Diptera, Simuliidae family), sand flies (SFs; Phlebotominae subfamily), and biting midges (BMs; Ceratopogonidae family, Culicoides). For each group, only a few species have been proven capable of amplifying and transmitting VSV (Rozo-Lopez et al., 2018). Vector–habitat identification for outbreak locations was based on one or more of these species for the three groups. BF larvae of the *Simulium vittatum* species complex are mainly found in flowing rivers and streams (Adler et al., 2004), whereas the semiaquatic BM larvae of *Culicoides sonorensis* are found in moist substrates such as muddy banks, wet ground, tree holes, or feces (Mullen & Murphree, 2019). The terrestrial larvae of SFs *Lutzomyia shannoni* are found in very dry areas

and deciduous forests (Ready, 2013). Each vector has a geographic distribution encompassing large portions of the western US. Species distributions are defined by suitable habitat and climate, but insect population abundance is typically influenced by weather. High populations of vector insects typically result from a seasonal weather pattern, such as a prolonged heat wave or precipitation event, and this can result in an outbreak if a virus is introduced to the region (Oliveira et al., 2020). Vector insects, along with the presence and density of susceptible animal hosts, contribute to conditions supporting potential VS outbreaks. One risk factor for VS outbreaks in the US is the long-dispersal distance, often enhanced by high-wind events, of insect vectors (Burgin et al., 2013; Sellers & Maarouf, 1990). There is strong evidence that overwintering occurs during outbreak cycles in the US (Palinski et al., 2021; Perez et al., 2010). Further studies are needed to determine the mechanisms and specific role of insect vectors during overwintering events. However, transovarial and venereal transmission has been experimentally demonstrated in BF and BM vectors (Drolet et al., 2005). The current paper focuses on the vector–environment relationships of three competent VSV insect vectors.

Hydrology and vector-borne diseases

Hydrology can be an important factor in elevated vector-borne disease risk (Walsh & Webb, 2018). Various hydrologic factors are associated with the immature stages of specific vectors, such as flowing water as preferred habitat for BFs and moist substrate as preferred habitat for BMs. Thus, there is an inherent relationship between hydrologic habitat and vector location, enhancing or restricting their ability to serve as a viable vector in specific locations. VS incidents are distributed near flowing water, with 72% of cases within 1 km of lotic habitat and the closest VS incidents to lotic habitat occurring in the spring (Elias et al., 2019). In addition to where VS incidents occur, streamflow is associated with temporal aspects of VS incidents. All first incidents in an area occur after peak annual streamflow and 89% of these occur after streams return to baseflow conditions (Elias et al., 2019). Although proximity to water is associated with VSV (Duarte et al., 2008; Hurd et al., 1999; McCluskey et al., 2003), the vector link is often missing because vectors are not collected at the location and time of outbreak investigations. Some field collections of vector species have tested positive for VSV, but their arthropods were found to be incompetent vectors in the laboratory (Mead et al., 1997). Given the likelihood of different vectors being involved in the transmission of VSV,

and that these vectors likely have differing ecologies, more research is needed on the hydrology–vector relationship and the geographic spread of vectors and disease during a VS outbreak.

Hotspots in disease mapping

Landscapes and landscape attributes influence spatial variations in disease incidence. A dynamic analysis including spatial and temporal interactions is recommended to better understand disease transmission (Lambin et al., 2010) and can be furthered by hotspot analysis. Hotspots colloquially refer to areas experiencing a phenomenon of high intensity. The hotspot analysis in spatial modeling is a statistical method that lends a definition of hotspots in spatial data by identifying spatially dependent clusters with relatively higher density when compared with the global response (Getis & Aldstadt, 2004; Getis & Ord, 1992; Ord & Getis, 1995). Hotspot analysis has had disease mapping applications throughout its development (e.g., AIDS incidence in Ord & Getis [1995]), including vector-borne diseases such as dengue (Getis et al., 2010). More recently, hotspot analyses have been applied in natural resources and agricultural research, including mapping forest health (Fei, 2010; Harris et al., 2017), vineyard disease (Cohen et al., 2011), pest infestation in crops (Al-Kindi et al., 2017), and livestock disease (Kracalik et al., 2013; Sumaye et al., 2013). The benefit of applying a hotspot analysis to VS incidents is that it delineates subsets of the environment conducive to disease for comparison across the western US. Additionally, due to vector mobility, the environments surrounding the VS-infected locations should be considered when assessing VS risk (Peck et al., 2020), reaffirming the utility of hotspot analysis to define the spatial footprint of surrounding areas for monitoring and comparison.

Objectives

Here we investigated the habitat–vector associations by relying on expert knowledge and previous research investigating hydrology and vector-borne diseases. We hypothesized that the likely insect vectors (BF vs. BM vs. SF) vary by habitat in VS hotspots across the western US. This analysis builds upon previous work identifying environmental conditions related to VS distribution by identifying vector–habitat characteristics in VS hotspots. Our specific objectives were to determine: (1) How regions of reoccurring VS differ from the rest of the western US? (2) How geographically separated regions of

interest (ROIs) and hotspots are similar temporally (across months)? (3) How vector–environment habitat a priori knowledge relates to observed hotspots? Identifying hotspots for VS provides an ability to ascertain key habitat–vector relationships in these areas. This may provide information regarding the predictive ability of these areas to aid managers in proactively implementing mitigation strategies (Peck et al., 2020).

METHODS

Study area

The full extent of the study area was determined by the contiguous watersheds at the hydrologic unit code (HUC) 4 level in the western US where VS occurred between 2004 and 2015, as defined in the study by Peters et al. (2020) (Figure 1a).

Hotspots

Using VS disease incidence and host distribution data to define hotspots

VS case-count data at the premises level were provided by the USDA Animal Plant Health Inspection Service (APHIS). A premise was defined as the physical site or property where the subjects of an investigation were located. In the US, accredited veterinarians are required to report cases of any livestock with vesicular lesions for investigation of potentially high-consequence regulatory diseases including VS. Regulatory officials then visit the premises, examine the animal(s), issue a quarantine, and collect diagnostic samples for confirmatory testing. Diagnostic test results are available online (US Department of Agriculture, 2020). VS disease incidence data in this analysis were limited to equine premises (Figure 1a). Although VS can affect a variety of livestock, most of the reported incidents in the US concern equines.

Host data were obtained from the national county-level horses and ponies inventory data from the National Agricultural Statistics Service (NASS, 2017). Data were obtained from the 2002, 2007, and 2012 censuses, which had occasional missing data in some years, so the three censuses were averaged by county (*sensu* Peters et al., 2020). Horse counts were then divided by county area to yield horse density (number of equine per square kilometers) and rasterized for the full study extent.

To quantify where VS cases were clustered during the 2004–2005 and 2014–2015 outbreaks, the local Getis–Ord

statistic, G_i^* (Ord & Getis, 1995) was calculated using the *spdep* R package (Bivand et al., 2013). This hotspot analysis was performed for every month during the two outbreaks with at least 10 equine VS premise records. Premise counts were aggregated to an 8-km grid, a cell size to group multiple local premises, covering the extent of all premises and normalized to the equine population by dividing case counts by horse density. The G_i^* statistic was calculated for every cell in the grid using three neighborhood distance thresholds: 7.9, 11.3, and 25.3 km. These distances are larger than the typical dispersal distance for BM and SF, but less than the typical BF dispersal distance. Wind can increase the dispersal distance (Burgin et al., 2013). These distances were chosen to ensure neighborhoods of cells with radii of 1–3 cells away from the center cell, with the shortest distance ensuring at least eight neighbors, the lower limit for to approach normality (Ord & Getis, 1995). A significance level of $\alpha = 0.05$ was used with the Bonferroni-corrected critical value of 4.77 (Ord & Getis, 1995). For each cell, the G_i^* values from the three distance thresholds were compared and the G_i^* value was kept from the largest critical distance with strictly increasing G_i^* values with increasing distance (Getis & Aldstadt, 2004). Cells with G_i^* values above the critical value are considered members of a hotspot.

Identifying counties and delineating ROIs

Counties

Because VS warnings are issued at the county level, considering which counties repeatedly emerge as VS nidus provided a study focus. The focal study areas were determined by first identifying which counties in the western US had the most VS cases in the 2004–2005 and 2014–2015 outbreaks. The states with cases in similar areas during the two outbreaks were Texas (TX), New Mexico (NM), Colorado (CO), and Wyoming (WY). For each of these states, we summed the number of equine cases per county and year. For each year and state, we selected the counties with the highest case counts. If the selected counties had high case counts for their state for at least two years out of 2004, 2005, 2014, and 2015, we considered them focal counties to study. Multiple counties adjacent to each other with similarly high case counts were analyzed together. Geographically separated counties with similarly high case counts within a state over multiple years result in multiple focal counties for the state. Counties with high and repeated VS cases were Fremont, Goshen, and Platte in WY; Larimer, Weld, Boulder, Delta, and Mesa in CO; Valencia and Bernalillo in NM; and Bastrop and Travis in TX

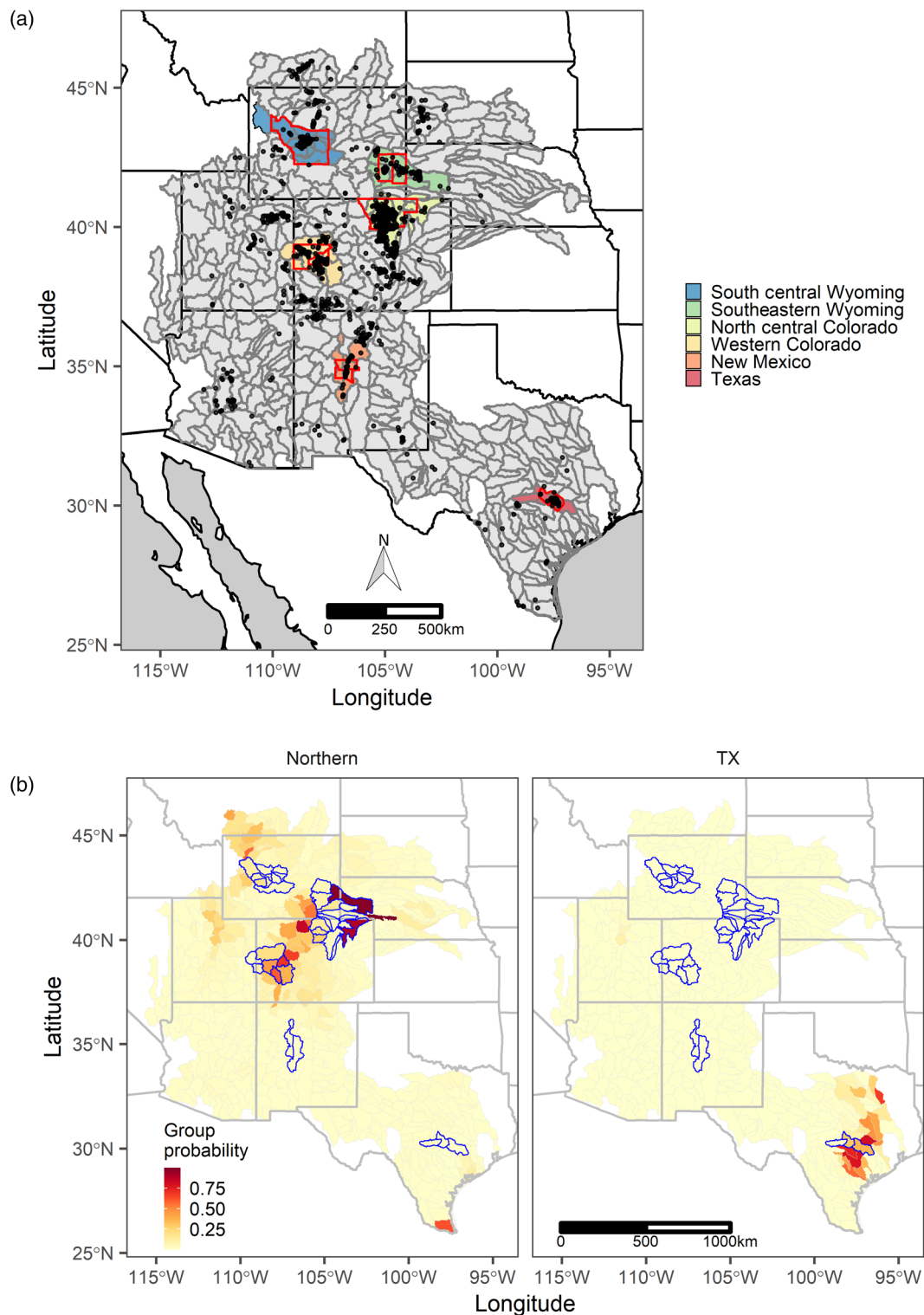


FIGURE 1 (a) The full study extent and six regions of interest (ROIs) of reoccurring vesicular stomatitis (VS) in this study. The contiguous watersheds comprising the full study extent are shown in gray. Red borders outline the focal counties. Each colored polygon represents an ROI. Points denote equine VS cases during the 2004–2005 and 2014–2015 outbreaks. (b) Group probability of watersheds for the northern and Texas (TX) groups. In the multivariate analysis of watershed characteristics, principal components (PCs) 1–16 were needed to explain 95% of the variance, indicating that watersheds composing ROI contain multivariate variability. For context, PC1 was generally a high livestock, high hay/pasture, high perennial lake, but low shrub/scrub axis, while PC2 was primarily a high irrigation, high cultivated crop axis. However, these PCs (which together only explain ~38% of the variance) do not separate the ROI watersheds from the broader western US. These primary differences across the western US do not distinguish ROI.

TABLE 1 Focal counties' region of interest (ROI) size and vesicular stomatitis (VS) case count from 2004–2005 and 2014–2015 outbreaks.

Focal counties	ROI	ROI area (km ²)	No. equine VS case counts in ROI per year			
			2004	2005	2014	2015
Fremont	SC-WY	27,550	...	23	...	70
Goshen and Platte	SE-WY	32,093	...	22	...	75
Larimer, Weld, and Boulder	NC-CO	35,490	99	1	281	111
Delta and Mesa	W-CO	31,999	3	49	...	134
Valencia and Bernalillo	NM	13,789	33	7	...	5
Bastrop and Travis	TX	12,191	...	1	44	...

Abbreviations: NC-CO, north central Colorado; NM, New Mexico; SC-WY, south central Wyoming; SE-WY, southeastern Wyoming; TX, Texas; W-CO, western Colorado.

(Table 1, Figure 1a). Although these focal counties were not the only counties in these states with VS cases in different years (e.g., west TX also has a case history), the selected counties serve as representative focal areas throughout the western US.

Watersheds

Due to the relationship between VS incidence and hydrological conditions (Elias et al., 2019), ROIs encompassing the focal counties were defined by watersheds (8-digit hydrologic unit code, HUC8) that intersect the focal counties (Table 1, Figure 1a). Watersheds that only partially intersected a focal county, and had a different HUC4 level than the other intersecting HUC8 watersheds, were not included (e.g., the watershed intersecting the northwest corner of north central Colorado [NC-CO]). All comparisons were made between ROIs since each ROI represents a hydrologically connected, as opposed to administrative-/county-based, area for comparing environmental conditions. The watershed-based ROI definition assumes that hydrology is important in defining vector–habitat and may exclude watersheds with one or a few isolated VS case counts.

Environmental variables

Broadscale analysis to compare ROI with the western US

Environmental variables for the broadscale analysis included livestock densities, land-cover proportions, stream and lake densities, and irrigation methods at the watershed scale.

To estimate general livestock density, we used livestock county-level count data (cattle and calves inventory [hereafter called “Cattle”], cattle and calves operations with inventory [“Cattle ranches”], horses and ponies inventory [“Horses”], and horses and ponies operations with

inventory [“Horse ranches”]) from the NASS (2017) Census of Agriculture from 2002, 2007, and 2012. We averaged the three censuses for each county since there were occasional missing data in these censuses in some years. County-level count data were divided by county area to yield livestock densities that were spatially averaged to watersheds.

We used land-cover data from the 30-m resolution 16-class 2016 National Land Cover Database (NLCD, Dewitz, 2019; Homer et al., 2020) from Google Earth Engine (<https://earthengine.google.com/>). We summarized and presented the land-cover data by percent composition per watershed.

We extracted the stream types and lengths, as well as waterbody types and areas, from the National Hydrography Dataset (NHD) (USGS, 2020a) NHDFlowlines and NHDWaterbody features, respectively. The Watershed Boundary Dataset (USGS, 2020b) WBDHU8 feature provides watershed areas for analyses. We calculated stream densities for all canal-type flowlines, and each of the ephemeral, intermittent, and perennial stream-type flowlines by dividing the total stream length (in kilometers) by the watershed area (in square kilometers) per watershed. Similarly, we calculated lake densities for intermittent and perennial lake-type waterbodies by dividing the total lake area (in square kilometers) by the watershed area (in square kilometers) per watershed. We used irrigation acreage by method data (micro-irrigation, sprinklers, and surface flooding) at the county level from the USGS Estimated Use of Water in the United States in 2015 dataset (Dieter et al., 2018). Prior to the comparisons, we converted county-level irrigation acreage data to county proportions (in square kilometers) and spatially averaged them to watersheds.

Gridded data for finer scale and monthly hotspot and regional analyses

We used gridded data representing land cover, soils, vegetation, surface hydrology, and meteorology to compare

geographically distributed regions, estimate hotspots, and infer likely vectors. Similar to the watershed analyses (above), we used land-cover data from the NLCD dataset but kept it in its original 30-m resolution. We extracted the soil drainage class from the gNATSGO database from NRCS (Soil Survey Staff, 2020) and modified it to provide hydrologic conditions. The dominant soil component value per map unit polygon was rasterized to the 30-m grid provided within the database. We further summarized this layer into two layers: the combination of excessively drained and somewhat excessively drained into a “dry” layer, and poorly drained and somewhat poorly drained into a “wet” layer. The very poorly drained class was not included to limit soils prone to ponded water at the surface. This soil drainage class was used instead of available water holding capacity since it encompasses soil properties, slope, and long-term meteorological conditions. We used normalized difference vegetation index (NDVI) data from MODIS at 250-m resolution (Didan, 2015) that were downloaded from Google Earth Engine (collection id: MODIS/006/MOD13Q1) as monthly mosaics of the 16-day product and then resampled to 30-m resolution.

We used the Global Surface Water (GSW) dataset to represent monthly surface water (JRC, 2020; Pekel et al., 2016). Monthly, remotely sensed surface water layers were downloaded by HUC8 watersheds via Google Earth Engine (collection id: JRC/GSW1_1/MonthlyHistory) and mosaicked locally. We calculated the distance to wetted ground gridded layer in Geospatial Data Abstraction Library (GDAL, GDAL/OGR Contributors [2020]) with distances up to 5 km. We estimated a dry ground monthly layer by identifying the pixels that were not detected as surface water or wetted ground.

Monthly streamflow was estimated by combining the NHD (Model Version 2.2.1) static NHDFlowlines layer with the GSW dataset. The flowlines were cropped to each ROI and rasterized to 30-m resolution. First, we estimated the monthly flowing water layer by each stream segment intersecting surface water per month. A monthly distance to flowing water was calculated with distances up to 15 km. Second, we created a modified version of distance to nutrient-rich flowing water by identifying streams within 1 km of expected nutrient-providing land uses (any of the four urban classes or cultivated crops), which also intersected the monthly surface water layer.

We extracted minimum monthly air temperature and average monthly vapor pressure from the Daymet v3 dataset (Thornton et al., 2018). Although the vector–environment literature provides ranges of hospitable relative humidity for SFs, these values were translated into vapor pressure using the Buck equation (Buck, 1981) and the accompanying temperature values, such that the indicator of atmospheric moisture was not a relative

value dependent on the temperature. These monthly layers were resampled to 30-m resolution.

Analysis by objective

How ROI differ from the broader western US (Objective 1)

To compare the ROI with the rest of the western US, we characterized watersheds in the full study extent by land-use proportions, livestock density, stream density, waterbody density, and irrigation proportions. For land use, we omitted the following classes as not indicative of vectors: barren land, mixed forest, herbaceous, open water, and evergreen forest. For this objective, we expressed all characteristic values as densities (in number per square kilometers) or proportions of a watershed to account for differences in watershed areas. Watershed characteristics were first compared univariately by their distributions of values per characteristic type (land use, livestock, streams, waterbodies, and irrigation). For each variable and ROI individually, the values for the ROI were compared with the values of the remainder of the study extent using a Wilcoxon rank-sum test and a significance level of $p \leq 0.05$. To also consider the multivariate characteristics of watersheds, the characteristics ($N = 22$) were individually centered, scaled, and then collectively analyzed via principal components analysis (PCA) using the R package *stats* (R Core Team, 2020). The minimum number of principal components (PCs) collectively explaining 95% of the variance was then treated as independent variables in a linear discriminant analysis (LDA) where the response variable was whether the watershed belonged to an ROI or not, using the R package *MASS* (Venables & Ripley, 2002). We also analyzed subgroups of ROI watersheds (e.g., splitting the ROI into north vs. south or individual ROI), as response variables in case not all ROIs had the same distinguishing subset of watershed characteristics. The final LDA model that was parsimonious in group definition yet maximized the difference between ROI and the remainder of the study area was determined. Then the PC with the greatest coefficient for each discriminant axis was identified and the watershed characteristics with a loading absolute value >0.35 on those PCs were reported. These resulting watershed characteristics, associated with each group, represent the characteristics that distinguished the ROI watersheds from the remainder of the full study extent. For each watershed, we used the posterior probabilities of belonging to each group provided by the final LDA model to ascertain the certainty of watershed similarity in space.

Comparing geographically separated regions and hotspots over time (Objective 2)

For this objective, data layers were preprocessed into vector–environment variables of interest (Table 2), rasterized to 30-m spatial resolution, and clipped to the ROI boundaries. For each ROI and month, environmental variables were compared between the hotspots within the ROI and with the whole area of the ROI. Even for static variables that do not change on a monthly basis (e.g., soil drainage class), hotspot summary values per month can vary because the area defined as a hotspot can change each month. First, mean values in the whole ROI were calculated and compared across months, years, and ROI (or just ROI for static variables) to indicate the variability of each environmental layer within and among ROI. Second, we used PCA to describe the multidimensional variability among hotspots, ROI, months, and years to indicate how hotspots vary from their own ROI and with hotspots in other ROIs in terms of the monthly mean environment subspace they occupy. We also calculated land-use preference by hotspots compared with their ROI by finding the difference in land-use proportions between hotspots and their ROI.

Using vector–environment a priori knowledge to estimate hotspots and likely vectors (Objective 3)

Defining vector–habitat relationships with a priori knowledge

Expert knowledge and scientific literature informed the selection of variables to describe the likely habitats associated with each vector. We defined a range of threshold values for each environment–vector relationship (Table 2). Thresholds were incorporated as ranges to account for uncertainty in the vector–environment relationships.

Many different insect species have tested positive for VSV during reported outbreaks, including BMs, BF, and SFs (Rozo-Lopez et al., 2018). However, the actual vectors during an outbreak have not been definitively identified, and some species that tested positive from wild populations were not found to be competent in VS transmission in the laboratory. The lack of robust ecological data related to potential vector species further complicates our understanding of vector transmission. To estimate habitat maps for potential vectors, we used ecological data from one well-characterized species from each vector family or subfamily (BM, BF, and SF), supplemented with data from other species of that family when necessary.

One of the most important BMs in North America is *C. sonorensis*. This species is frequently associated with livestock, and often breeds in mud organically enriched from manure, but it also occurs in other environments. *C. sonorensis* is a competent laboratory vector of VSV (Drolet et al., 2005; Perez De Leon et al., 2006; Perez de Leon & Tabachnick, 2006) and wild populations have tested positive during outbreaks (Rozo-Lopez et al., 2018). To map likely habitats, we used literature-derived dispersal information. BMs are weak fliers and generally do not disperse more than 1.8 km from their natal habitat (Lillie et al., 1981).

Except for a few rare instances, BF develop in lotic habitats, from ephemeral streams and seeps to larger rivers. Various hydrological and environmental variables are related to BF presence–absence and abundance. Because ecological knowledge for many species is sparse, the parameters for initial inclusion in the model were based on the ecology of the *S. vittatum* species complex, one of the better-studied BF species and known competent vector (Mead et al., 1999). Species of the *S. vittatum* complex are found in waterways throughout North America and can be quite abundant under suitable conditions. BF have excellent dispersal with some species traveling 225 km (Fredeen, 1969), but more commonly less than 15 km (Baldwin et al., 1975; Bennet, 1963; Moore & Noblet, 1974). Mark–recapture studies of *Simulium venustum* found an average emigration distance between 9.3 and 13.1 km (Baldwin et al., 1975). Abundance of food and food quality are important predictors of BF abundance (Gislason et al., 1994; Morin & Peters, 1988; Stone & Snoddy, 1969). BF larvae filter feed on suspended microbes, algae, and detritus from the water; the abundance and quality of these food sources are directly related to nutrient input, such as runoff from agricultural areas or river impoundments (Gislason et al., 1994; Morin & Peters, 1988; Stone & Snoddy, 1969). The influence of such nutrient sources wanes at approximately 1 km downstream from the source (Morin & Peters, 1988). Riparian habitat can be important as well. *S. vittatum* is more likely to be found in streams and rivers without dense overhanging forests as females rely on oviposition pheromones to communally lay eggs on trailing vegetation (Adler & Kim, 1984).

Phlebotomine SF larval habitats are dry areas without aquatic or semiaquatic habitats or seasonal precipitation. Phlebotomine larval habitats are inconspicuous and consequently little is known about the immature stages. Most habitats are found using emergence trapping (collecting newly emerged adults) or using eDNA (finding evidence of SF DNA in the soil samples). Although there are approximately 900 species of phlebotomine SFs, only a few are proven VSV vectors. The most significant

TABLE 2 The environmental data used to compare region of interest, their sources, and their relevant vector.

Variable	Native spatial resolution	Source/cite	Vector	Threshold	Vector–environment reference
Monthly (distance to) wetted ground: water detected last month but not this month	30 m	Calculated from GSW dataset's monthly water history layer (Pekel et al., 2016)	Biting midges	<0.8–2.11 km with an average of 1.8 km	Lillie et al. (1981)
Monthly (distance to) flowing water: reaches intersecting detected monthly surface water	Flowlines	Rasterized static NHD flowlines (US Geological Survey, 2020a) and intersected with monthly GSW	Black flies	<10–15 km	Bennet (1963), Moore and Noblet (1974), Baldwin et al. (1975)
Nutrient-rich water: reaches within 1 km of developed land or cultivated crops	Flowlines	Rasterized static NHD flowlines, intersected with NLCD and monthly GSW	Black flies	<10–15 km	Range same as above; Morin and Peters (1988)
Monthly dry ground	30 m	Absence of wetted ground, surface water, or flowing water	Sand flies	...	Young and Duncan (1994)
Monthly mean minimum air temperature	1 km	Daymet v3 (Thornton et al., 2018) https://daymet.ornl.gov/	Biting midges; black flies; sand flies	Midges: >10–14°C; black flies: >12.8°C; sand flies: >22–27°C	Mayo et al. (2014), Adler et al. (2004), Ferro et al. (1998)
Monthly mean vapor pressure	1 km	Daymet v3 (Thornton et al., 2018) https://daymet.ornl.gov/	Sand flies	>2300–3693 Pa	Estimated from relative humidity and air temperature from Ferro et al. (1998)
Land cover	30 m	National Land Cover Database (Homer et al., 2020) https://www.mrlc.gov/	Sand flies	Deciduous tree holes	Weng et al. (2012), reviewed by Munstermann (2005), Ready (2013)
NDVI	250 m	MODIS (Didan, 2015)	Biting midges	>0.05–0.15	Baylis et al. (1998), Diarra et al. (2015)
Poorly draining soil: drainage class as poorly or somewhat poorly drained; Well-draining soil: drainage class as excessively or somewhat excessively drained	30 m rasterized soil map unit polygons	NRCS gNATSGO (Soil Survey Staff, 2020)	Biting midges; sand flies	...	Mullen and Murphree (2019), see review by Ready (2013)

Abbreviations: gNATSGO, gridded National Soil Survey Geographic Database; GSW, Global Surface Water; MODIS, moderate resolution imaging spectroradiometer; NDVI, normalized difference vegetation index; NHD, National Hydrography Dataset; NLCD, National Land Cover Dataset; NRCS, Natural Resources Conservation Service.

SF vector in the US is *L. shannoni* that is commonly associated with hardwood deciduous forests. Currently, reports on the presence of *L. shannoni* include 14 US states (only one western state though—Alabama, Arkansas, Delaware, Florida, Georgia, Louisiana, Maryland, Mississippi, North Carolina, South Carolina, New Jersey, Kentucky, Ohio, Tennessee, and Texas) (Claborn et al., 2009; Comer et al., 1990; Haddow et al., 2008; Minter et al., 2009; Price et al., 2011; Young & Perkins, 1984). *L. shannoni* are found in tree rot holes and rodent burrows. SFs are considered weak fliers and typically have low dispersal distances of 100–150 m; however, some species travel up to 1 km when seeking hosts (Young & Perkins, 1984).

Estimating habitat maps using a priori knowledge

Vector-habitat maps were constructed by comparing each monthly geospatial layer to its threshold range (Table 2). We assigned a marginal suitability score between 0 and 1 based on its location in that threshold range (e.g., 0 if less than the lower threshold minimum; 1 if greater than or equal to the lower threshold maximum). If the value was two-thirds between the lower threshold minimum and maximum, we assigned a 0.66 value. We averaged the marginal suitability scores among all variables for each vector to estimate a suitability score per vector for each pixel. These suitability scores represent our a priori knowledge of vector-habitats. The suitability scores were depicted geographically using the acquired geospatial environmental data as habitat maps. Thresholds used a parsimonious way to represent our limited knowledge of the marginal vector-environment relationships. They are Bernoulli distributions, as opposed to a regression relationship that would be feasible only with more vector presence or abundance data. Ranges of thresholds allowed us to incorporate our uncertainty about these thresholds. The *p* parameter of our Bernoulli distributions is unknown, so we sampled from our threshold ranges as if they were uniform prior distributions in a Bayesian context. Similar deductive suitable habitat modeling approaches have been used when species occurrence data are sparse, such as the process used to develop species habitat models in the USGS GAP analysis project (Gergely et al., 2019).

Comparing vector-habitat maps to hotspots

After we estimated monthly VS hotspots and vector-habitat maps independently, they were compared to indicate likely vectors (BF vs. BM vs. SF) among ROI and hotspots across time. First, each ROI as a whole and their associated hotspots was summarized by the 25th, 50th, and 75th percentile suitability score

per month to indicate the spatial variability of scores. Additionally, each region-month habitat suitability score map was converted to a categorical suitable/non-suitable map using a cutoff suitability score of 0.5 to indicate where there was at least half confidence that the environment would support the vector given our a priori knowledge. These individual categorical suitable habitat maps were summarized by their mean habitat patch size, both for the ROI and only hotspots, per month to indicate the degree of vector-habitat aggregation. Habitat mean patch size was calculated by the *landscapemetrics* package (Hesselbarth et al., 2019). We further categorized each pixel into unique combinations of supported vectors using the intersection of the three categorical suitability vector maps per ROI and month to indicate where multiple vector-habitats overlap in space. The eight unique combination categories were no vectors, only BM, only BF, only SF, both BM and BF, both BM and SF, both BF and SF, and all three BM, BF, and SF. For each ROI, hotspot, and month, we calculated the percentage area fitting into each category to indicate when and where individual and multiple vectors had suitable environments. We used the GDAL (GDAL/OGR Contributors, 2020) and Google Earth Engine (Gorelick et al., 2017) for geospatial processing and R for data manipulation, statistical tests, and visualizations (R Core Team, 2020).

RESULTS AND DISCUSSION

How ROIs differ from the broader western US (Objective 1)

Individual environmental factors

Livestock density, hydrology, and irrigation were expected to correlate with ROI; however, no single, independent factor explained the existence of VS in watersheds of each ROI compared with the rest of the western US. Livestock density was not consistently higher in ROIs compared with the broader western US (Figure 2), hence ROIs were not centers of VS solely because of a higher density of livestock hosts.

ROI watersheds, except for in TX and NM, had higher median canal densities than watersheds comprising the western US (Appendix S1: Figure S1). The ROI watersheds in western Colorado (W-CO) and south central Wyoming (SC-WY) had higher perennial stream densities than the rest of the spatial extent (Appendix S1: Figure S1). These streams would consistently provide conditions conducive for BFs. Ephemeral streams were the least persistent and likely the least relevant as vector-habitat for BFs since

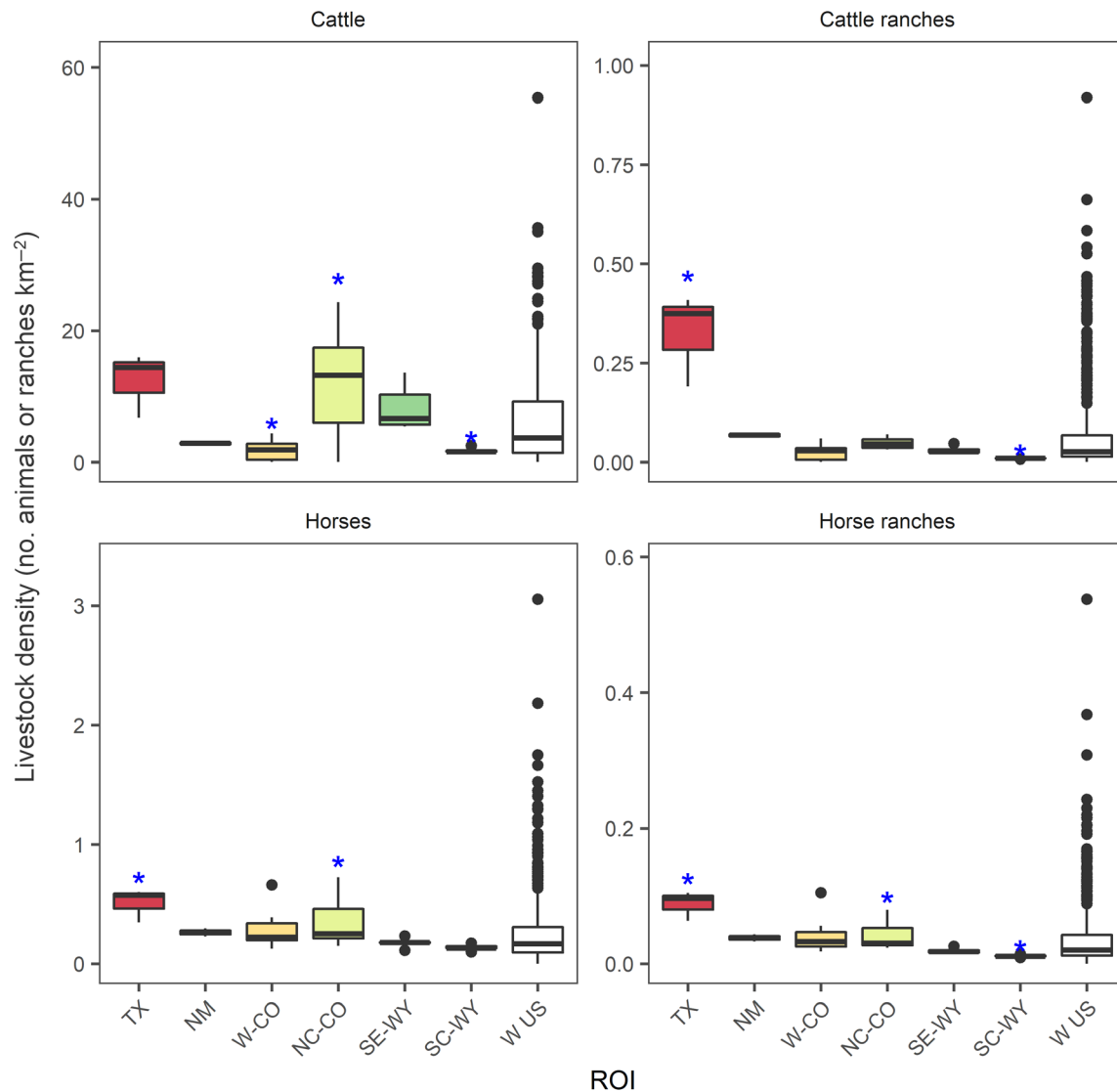


FIGURE 2 Livestock density in watersheds for the six regions of interest (ROIs) and the remainder of the full study extent representing the western United States (W US). Blue asterisks denote when the ROI has a significantly different rank sum than W US. NC-CO, north central Colorado; NM, New Mexico; SC-WY, south central Wyoming; SE-WY, southeastern Wyoming; TX, Texas; W-CO, western Colorado.

streamflow only occurs following precipitation events. The higher canal (four of six ROIs) and perennial stream (two of six ROIs) density in watersheds comprising VS ROI suggest that these water bodies may provide flowing water habitats beneficial to BFs. Higher canal density within ROI watersheds might also support BM habitat via wetted ground from irrigation.

Irrigation via canals and wetted ground may foster insect habitat. Irrigation by surface flooding could be supportive of longer-term wetted ground required for BM habitat. Irrigation methods and extents vary among the watersheds (Appendix S1: Figure S2) with the TX ROI using a mix of all three methods; the NM, W-CO, and SC-WY ROI overwhelmingly using surface flooding; and the NC-CO and SE-WY ROI using a mix of sprinkler

and surface flooding. Surface flooding was significantly higher in the four ROIs with more canals (CO and WY ROI) than in the rest of the study area.

Watershed similarity

Multiple environmental factors were used to distinguish watersheds and ROIs. PCs grouped the northern ROI (those in CO and WY), NM, TX, and the remainder of the study extent. LDA was unable to distinguish NM from the remaining study extent; thus, NM was excluded from the northern and TX groups to retain their unique characteristics.

The probability of each watershed belonging to either the northern or TX group of watersheds indicates that

there are other nearby watersheds with similar combinations of characteristics as the two ROI-based groups (Figure 1b). The strongest group assignment was in a corridor across the northern region (Figure 1) including W-CO, NC-CO, and SE-WY ROIs, although some watersheds within these ROI have low group probability. The northwest boundary of our study area, including northeast UT and southern MT watersheds, had conditions similar to the W-CO/SE-WY corridor watersheds, but few VS occurrences. Reasons for the lack of observed VS cases in these watersheds could be related to variables not included here, such as temperature, or the inability of the virus

to reach these locations before the end of an expansion year. Watersheds adjacent to the TX ROI had similar characteristic combinations to those watersheds comprising the ROI (Figure 1). Historic records indicate some of these watersheds had VS, both in the 2004/2005, 2014/2015, and earlier outbreaks (Peters et al., 2018; Rodríguez, 2002).

The groups defined above resulted in three discriminant axes (LD1–3) used to differentiate those data. The percentage separation by each discriminant axis was 70.5% (LD1), 21.2% (LD2), and 8.3% (LD3). LD1 generally distinguished the northern group from the others.

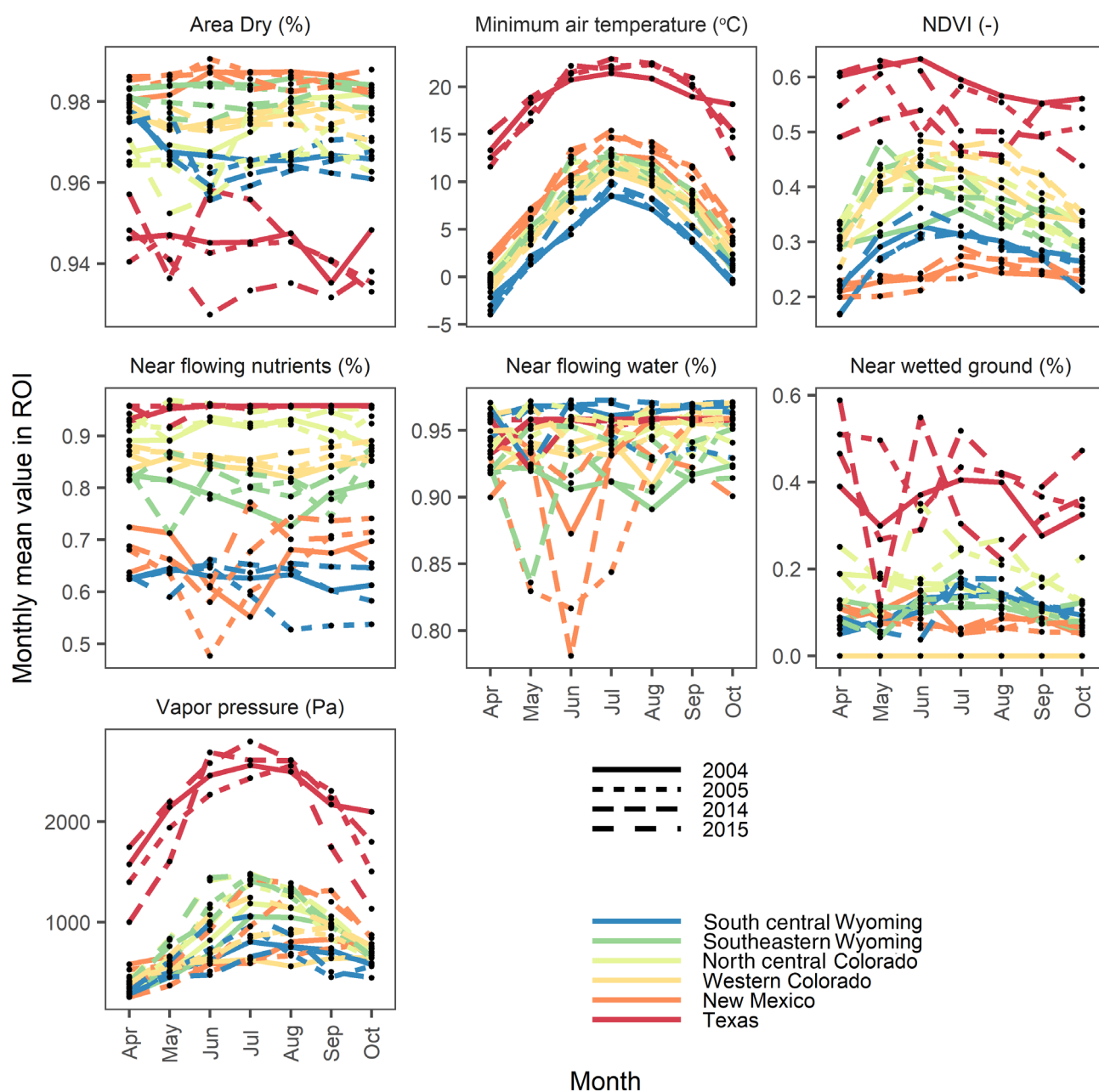


FIGURE 3 Monthly mean environmental values for the entire region of interest (ROI). Values used for proximity to hydrological conditions were the upper values specified in Table 2.

LD1 (northern group) is associated with PC3, indicating higher canal density and perennial stream density (Appendix S1: Figure S1), and higher proportional area with surface irrigation (Appendix S1: Figure S2). LD2 distinguished TX and was associated with PC15, indicating higher perennial lake density. Perennial lake density (PC15) was also correlated with horse, horse ranch, and cattle ranch density (PC1) (Figure 2). LD3 represented NM, but was poorly separated from the remainder of the study area via PC16, representing low cultivated crops and high shrub area.

The static analysis of watershed factors indicated a more complex system separating areas with high, recurring VS from the broader western US. Univariate analyses indicated that no single characteristic separated the six ROI from other areas, dispelling the myth that VS outbreaks occur merely due to high host density. Multivariate analyses indicated differences between ROI with two distinct groups emerging (northern ROI and TX). The static analysis of this objective was unable to comprehensively differentiate ROI from the broader western US with the characteristics that were considered. Finding no consistent watershed-scale

characteristics defining all ROIs, we next investigated vector–habitat with finer scale and transient features within ROIs.

Comparing environmental conditions among regions and hotspots (Objective 2)

Monthly mean values show variability in environmental conditions over time. Meteorological conditions in the ROIs tend to differ along their latitudinal gradient. The southernmost ROI (TX) had higher nighttime temperature and vapor pressure deficit with earlier spring, whereas the northernmost ROI (WY) had lower temperatures with later springs (Figure 3). TX had the highest proximity to wetted ground and nutrient-rich flowing water, the highest NDVI, the least dry area compared with the other five ROIs (Figure 4). Although the NM ROI was geographically nearest the TX ROI, it had distinctly different hydrological and vegetation conditions with low proximity to wetted ground, high monthly variability in proximity to and nutrient-rich flowing water, the most dry area, and low NDVI. Moving north, W-CO was

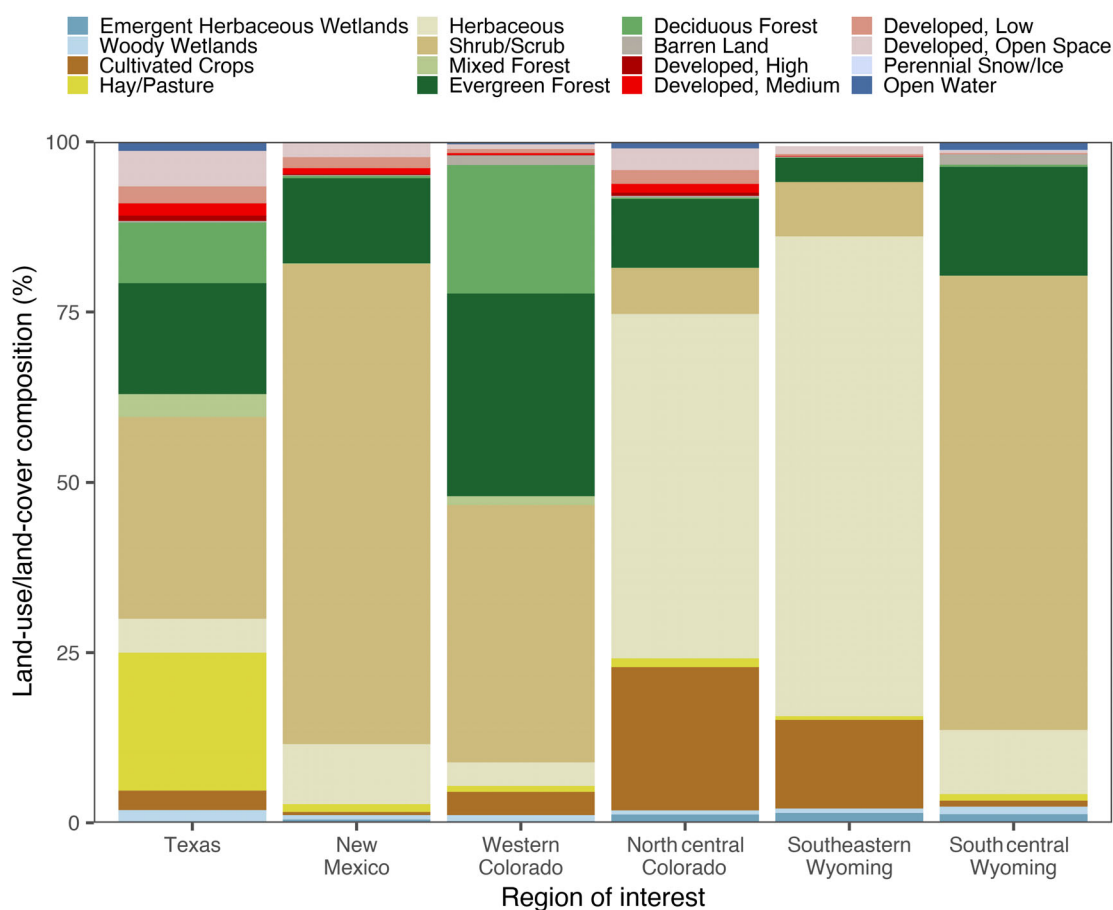


FIGURE 4 Land-use/land-cover composition for each region of interest.

distinguished by cooler temperatures, high summer NDVI, high deciduous forest cover, and seasonal NDVI variation. NC-CO was distinguished by having the most cultivated cropland cover (21.1%), higher proximity to nutrient-rich

flowing water, and wetted ground compared with other ROI. SE-WY had moderate proximity to flowing water and NDVI, and a high percent dry area and herbaceous land cover (70.4%). The northernmost ROI, SC-WY, had the latest

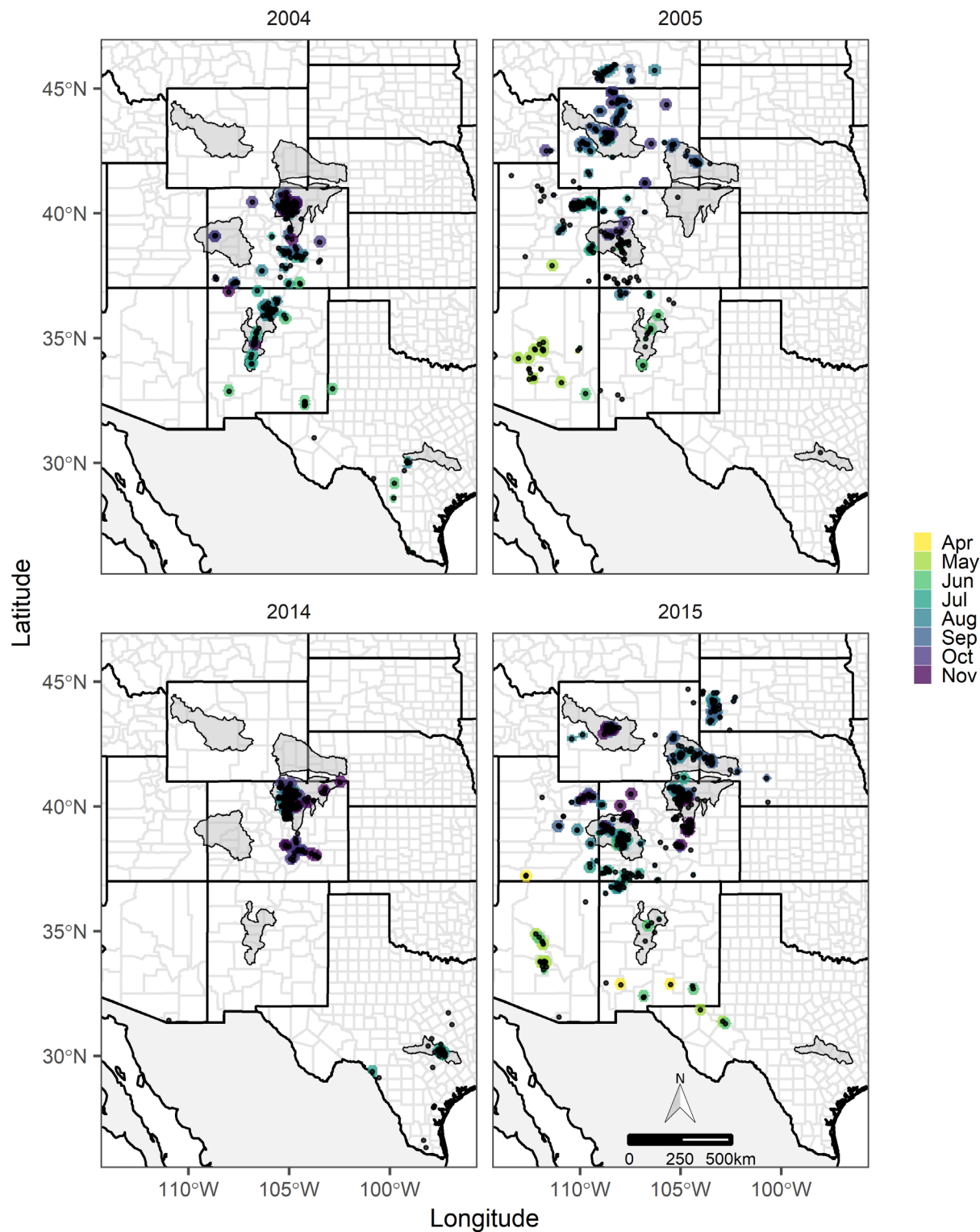


FIGURE 5 Monthly vesicular stomatitis (VS) hotspots in 2004, 2005, 2014, and 2015. Black points represent the equine VS cases in each year. Hotspots are defined by pixels with local Getis-Ord statistic G_i^* above the 95% confidence level threshold in a specific month. Hotspots are colored by their month of occurrence. Gray polygons delineate the six regions of interest.

spring, lowest nighttime temperatures, second lowest NDVI, and highest proximity to flowing water. Abrupt changes in monthly values for hydrological variables in some ROI (TX and NM) suggest that suitable conditions for specific vectors may change throughout the year. The environmental variability in differing ROI indicates that there may have been different vectors responsible for VS outbreaks at different times of the annual cycle and in different ROI.

Environmental conditions in hotspots

VS incidents first occurred in the south in April–June and the virus appeared in different locations over time, spreading northward and persisting through November (Figure 5). Hotspots during 2004 and 2014 tended to start later in the year (June), than those of 2005 and 2015 (May and April), respectively. The early April–May

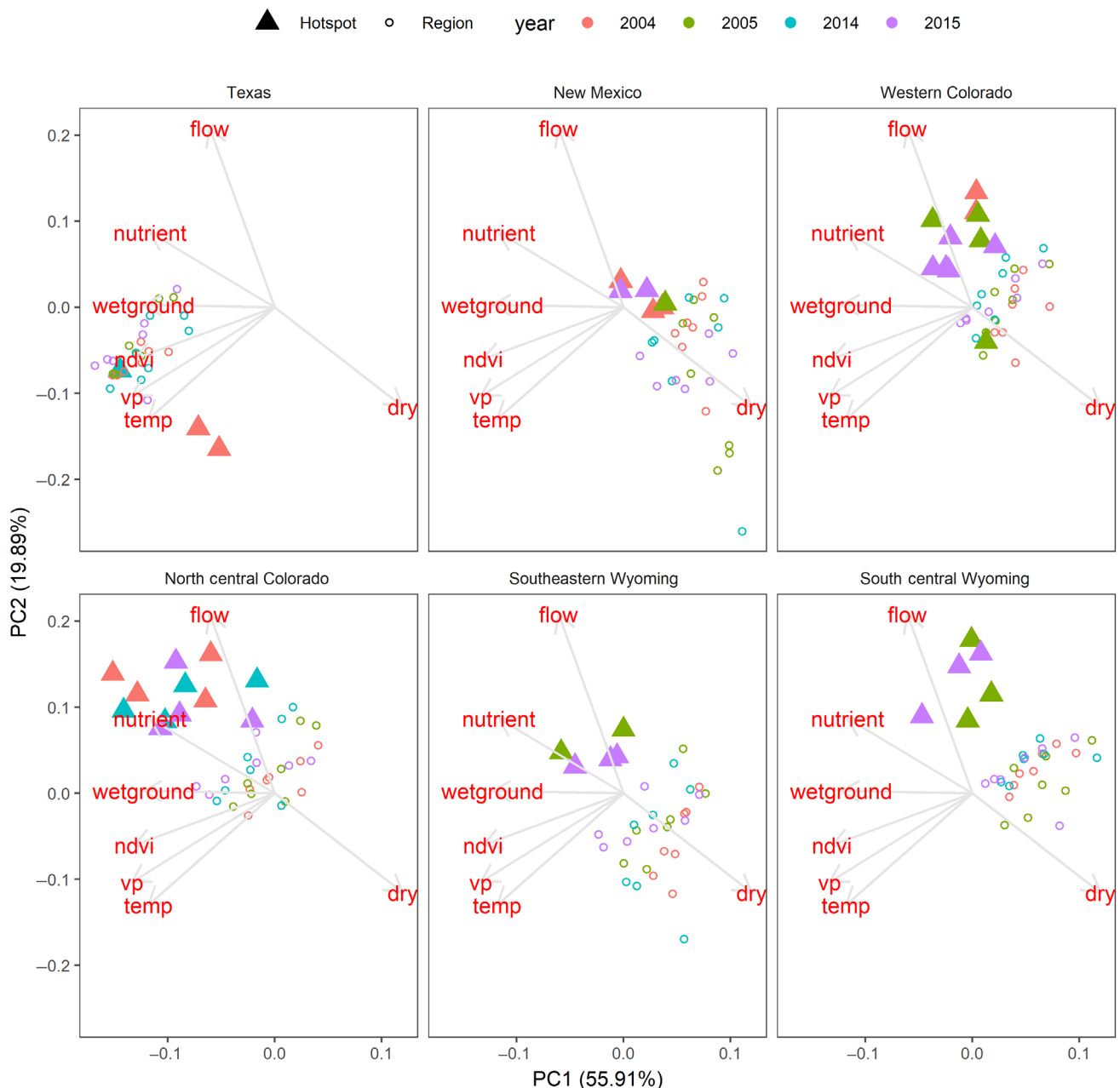


FIGURE 6 Principal components analysis of mean environment between hotspots and regions. Each open circle represents a month per region ($N = 28$, April–October for the four years), not including hotspot areas. Each filled triangle represents hotspot areas per month in the region (N is variable). For distance to water variables, the upper limit of their thresholds was used. NDVI, normalized difference vegetation index; temp, temperature; vp, vapor pressure.

hotspots in 2005 and 2015 occurred outside the ROIs. In the six ROIs, hotspots generally occurred from June to November. In 2004, ROI hotspots primarily occurred in NM and NC-CO, while in 2005 they primarily occurred in all ROIs except TX and NC-CO, exhibiting a westward shift. In 2014, ROI hotspots primarily occurred in TX and NC-CO, while in 2015 they primarily occurred in all ROIs except TX, exhibiting a broader total extent.

Comparing mean environment between hotspots and regions

All ROIs except TX had hotspots with closer proximity to flowing water on average than the region as a whole (Figure 6). In TX, hotspots occurred in drier conditions than the rest of the ROI in 2004, but similar to the region in 2014. Among the ROIs, hotspots in

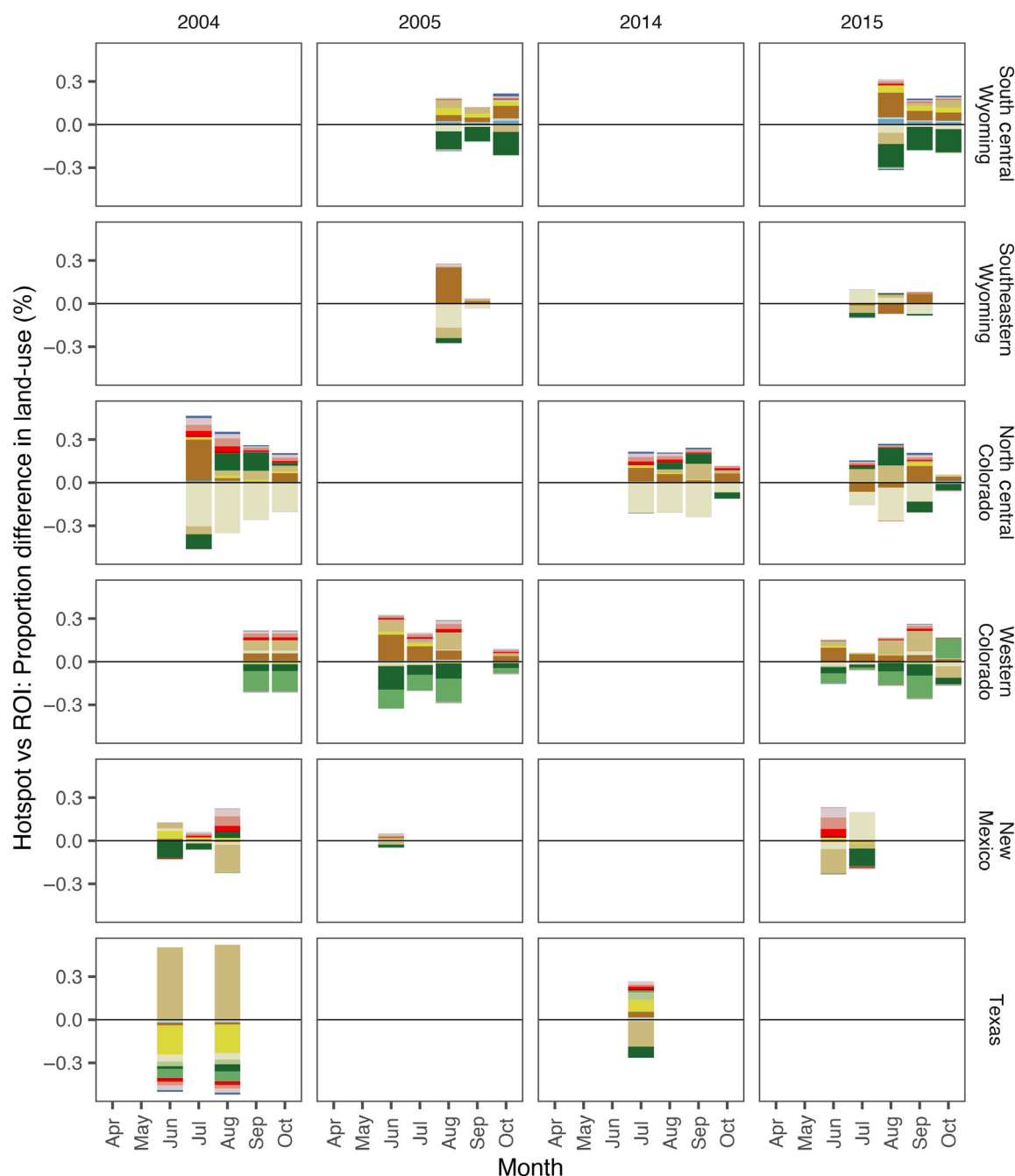


FIGURE 7 Differences in land-use proportions. Positive values: hotspots disproportionately occur in these land-use classes compared with the composition of the whole region. The magnitude of the columns reflects how different the hotspot proportions are from the whole region. Positive and negative values are always symmetrical within a month/region of interest (ROI) because one or more land-use classes in a hotspot displace the region's class proportionally. Color legend is the same as Figure 4.

NC-CO had the greatest amount of area close to nutrient-rich flowing water, followed by SC-WY, W-CO, and SE-WY. NM hotspots were moderate in hydrological conditions as indicated by their location near the origin.

Hotspots occurred in specific land-cover classes within an ROI in proportions similar to the ROI's composition (Figure 7). In general, hotspots in W-CO and SC-WY did not occur in forested areas, and hotspots in NC-CO did not occur in herbaceous cover.

Hotspot estimation allowed us to define areas (as opposed to points) to describe VS incidences in a given month. Hotspots first appeared in southern ROI and progressed northward throughout the year with the general flow of the VS outbreak. Environmental characteristics in hotspots differed from the broader ROI. In all ROIs except TX, hotspots tended to be closer to flowing water. Land-use composition in

hotspots also differed from the broader ROI. In five of six ROIs, hotspots tended to occur less in forested (except NC-CO) or herbaceous areas, and occurred more in available cultivated crops, shrub/scrub, and hay/pasture (except TX). While cultivated crops and hay/pasture comprised a smaller portion of land-use composition in each ROI, there was a tendency for hotspots to occur in these land-cover classes. Hotspots occurring in agriculture-related land uses may relate to livestock proximity.

Comparing hotspots and vector-habitats (Objective 3)

Using vector-environment knowledge allowed us to estimate hotspots and likely vectors. Suitability scores, calculated for each month, represent how suitable the

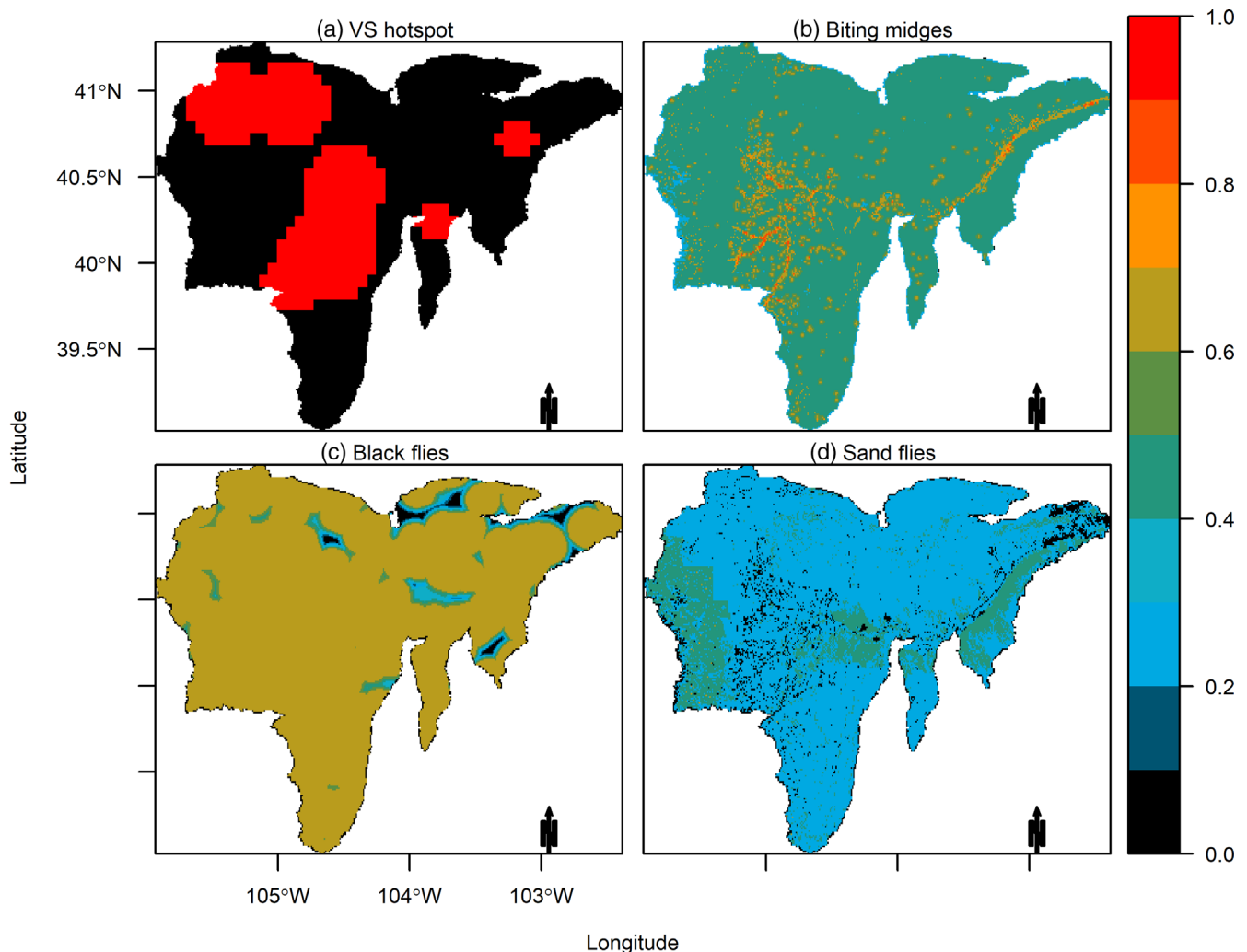


FIGURE 8 Vesicular stomatitis (VS) hotspot and marginal vector suitability scores in the north central Colorado region of interest for October 2014 as an example. For hotspots, values are limited to 0 for non-hotspot and 1 for hotspot. For marginal vector suitability scores, values 0–1 indicate the degree of suitability from not suitable to suitable.

environment was to support BM, BF, and SF habitat given our a priori vector–environment knowledge. The spatial depiction of suitability from October 2014

(Figure 8) indicated a 40%–50% probability of suitable BM habitat across the NC-CO ROI, with higher suitability along riparian corridors. BFs also had the highest

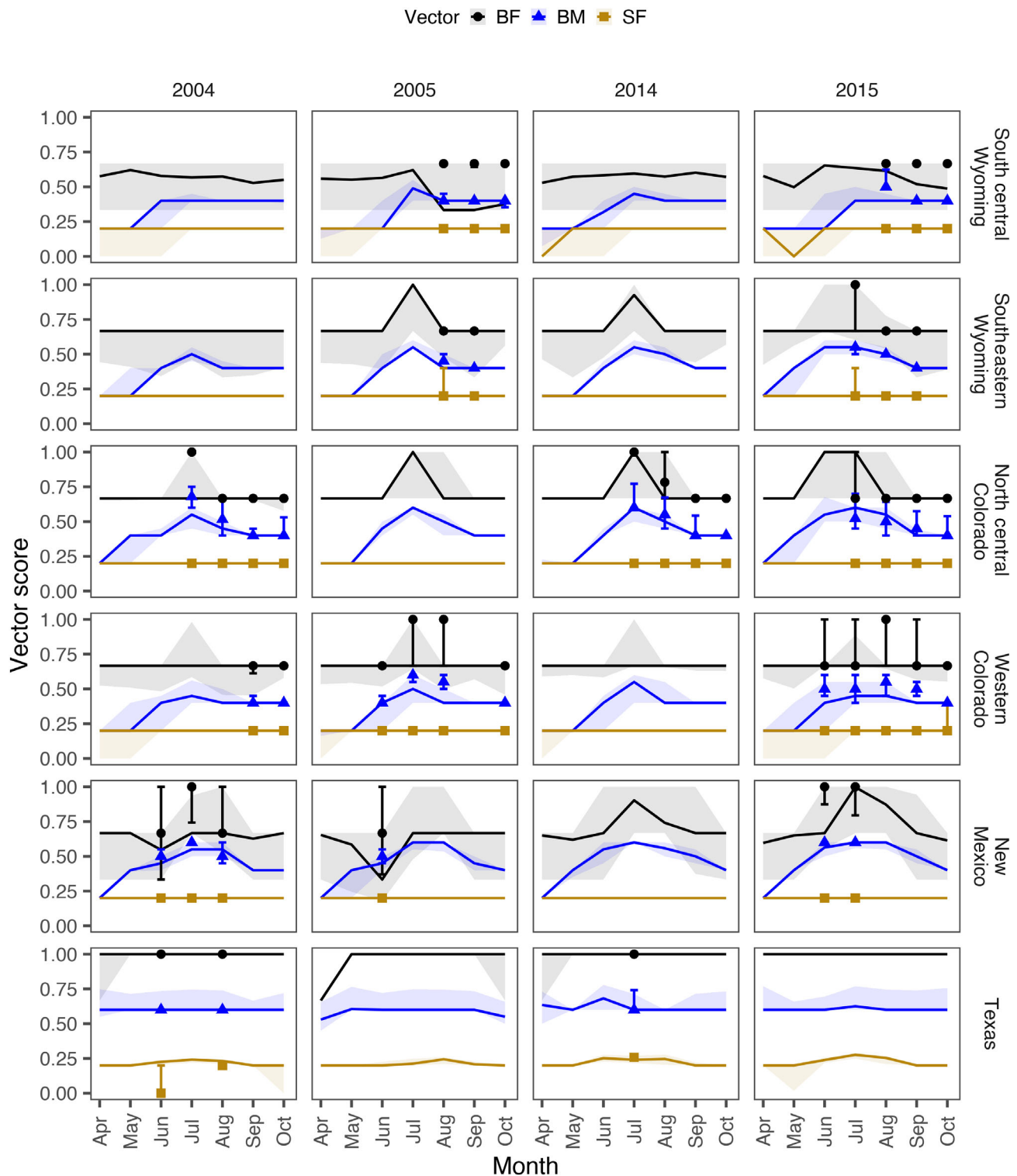


FIGURE 9 Monthly vector suitability scores in regions of interest and their hotspots per vector. Lines indicate the median with ribbons indicating the 25th and 75th percentile of suitability scores across the region. Symbols indicate the median with error bars indicating the 25th and 75th percentile of suitability scores within hotspots in the region. BF, black fly; BM, biting midge; SF, sand fly.

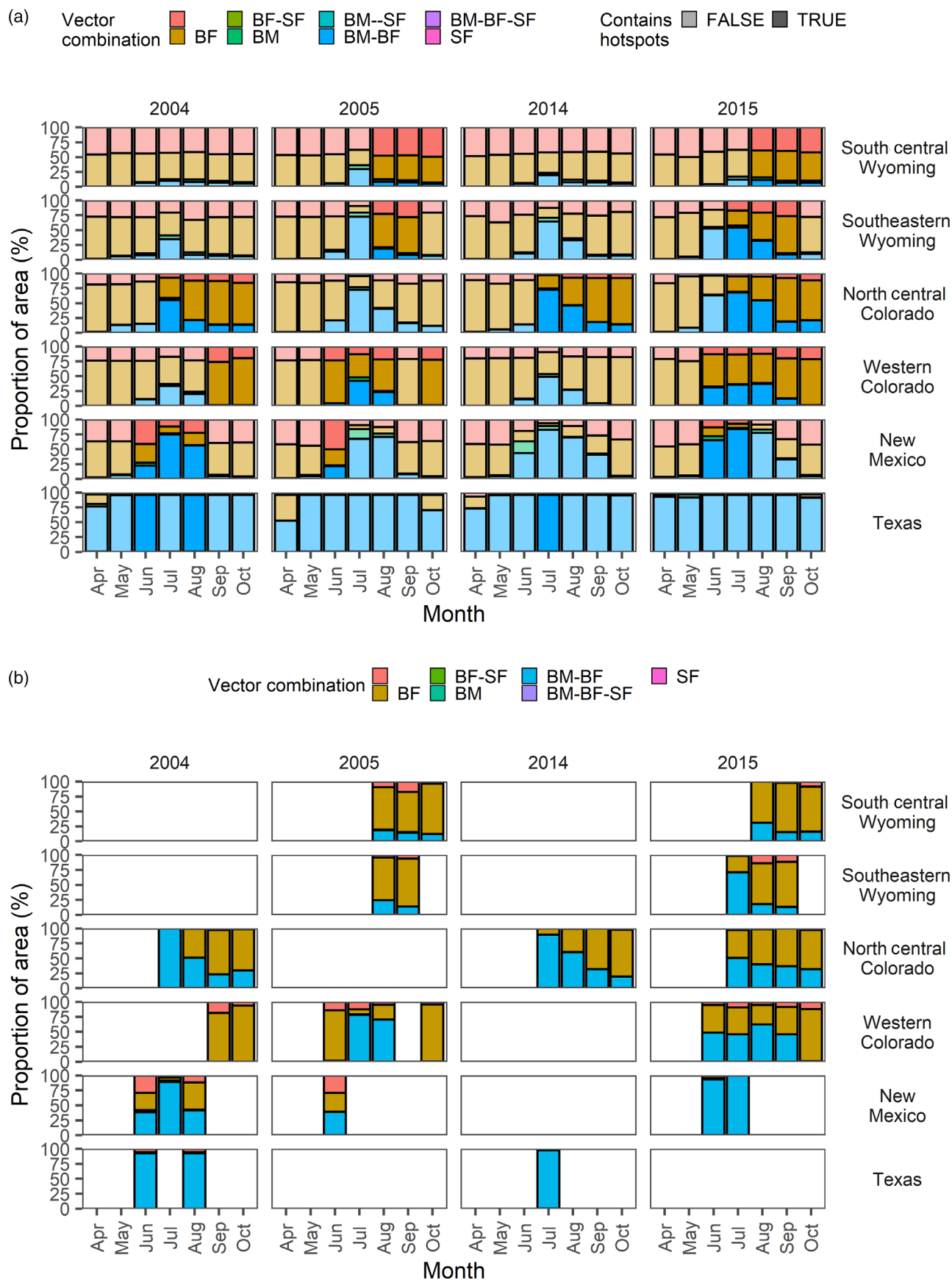


FIGURE 10 Legend on next page.

suitability across the NC-CO ROI for this month, and since the incubation period for VS is between 2 and 9 days, linking habitat with likely vector on a monthly time step is feasible.

All ROIs experienced environmental conditions suitable for multiple vectors at some point in the year (Figure 9). BFs had the highest suitability scores, whereas BM suitability scores were lower and varied annually with higher suitability in summer. SFs generally had the lowest suitability score in all regions. The southernmost ROI, TX, supported both BMs (~0.6 median suitability score) and BFs (~1.0 median suitability score) throughout April–October. By contrast, the northernmost ROI, SC-WY, supported BFs (~0.5 median suitability score) in the ROI throughout April–October and BMs after June (~0.4 median suitability score). NC-CO hotspots generally started occurring during the peak BM month of July, which coincided with the peak BF suitability score (~1.0), and persisted through October. Highly favorable conditions for both vectors may have contributed to VS hotspots persisting. NM hotspots began earlier in the year than CO and WY hotspots (before June), peaked in July, and did not persist through the year (Figure 10). For W-CO, hotspots started occurring in September 2004 after the environment was less suitable for BMs, then reappeared in June 2005 before the environment supported BMs (Figure 10a).

The monthly proportion of the ROI with suitability scores higher than 50% depicts likely vector combinations in ROI with and without hotspots, allowing estimates of likely vectors during outbreaks (Figure 10a). This approach does not allow estimating a single likely vector in TX where BM and BF habitat persisted and overlapped in nearly all of the ROI from April to October. By contrast, suitable BM and BF habitat varied monthly in the NM ROI, with some overlap. Some habitats were only suitable for BMs or BFs in June 2004, with the total suitable area at ~60%. Occasionally there was overlap in BM and SF habitat (e.g., NM 2005), but this rarely occurred within hotspots. When considering the vector–habitats only within hotspots, and not the broader ROI, at least one vector had a suitability score >0.5 in at least ~75% of the hotspot areas during hotspot months (Figure 10b). In SC-WY, hotspots had mostly BF suitable habitat and less BM and SF habitat. BM habitat during hotspots in WY and

N-CO tended to decrease over time, whereas BF habitat persisted.

To indicate the degree of vector–habitat aggregation, individual suitable habitat maps were summarized by their monthly mean habitat patch size, both for the region as a whole (Figure 11a), and within hotspots (Figure 11b). BM habitat patches were often orders of magnitude smaller than BF patch areas. This spatial difference relates to their shorter dispersal distances since the threshold distance to their preferred hydrologic condition, and not the presence of the condition alone, was used in the habitat definition. While there was a consistent patch size area for BF throughout the year, there was a seasonal pattern for the BM patch area (Figure 11a). Patch areas in hotspots further reinforce the likelihood that BF may be the most critical vector for VS in northern ROI, whereas both BM and BF have similar patches and likelihood in southern ROI (TX and NM; Figure 11b).

Given a priori knowledge of BF–environment relationships, most areas within ROIs and hotspots had BF suitability scores ≥ 0.5 . While this may relate to limited constraining knowledge, current expert opinion using the best available information indicated broad BF habitat. However, there was a latitudinal gradient in BF suitability scores, with lower suitability in northern ROI. Because BFs have the largest average dispersal distance (e.g., being able to move farther away from water) of the three vectors, they are less susceptible to habitat fragmentation. Mean patch size implies that BF suitable habitat is clumped into larger patches as opposed to many small patches since it was generally high and constant throughout the year and contained most of the hotspots. Based upon prior knowledge of BM–environment relationships, suitability scores varied throughout the year in most ROI with the exception of TX where scores were steady at 0.6. In hotspots, BM habitat typically decreased near the end of an outbreak in northern regions, whereas TX and NM had more consistent BM habitat. BM habitat patches showed similar seasonal patterns with a peak patch area in July and lower mean patch areas in April and October in most ROI. SF–environment relationship suitability scores were very low, with generally less than 1% of ROI area suitable, indicating they are an unlikely VS vector in the ROIs and hotspots investigated.

FIGURE 10 (a) Monthly proportion of region of interest (ROI) area with combinations of vectors with suitability scores ≥ 0.5 . Fill colors represent unique vector combinations. Opacity represents whether the ROI contains hotspots (dark) or not (light) during the month. (b) Monthly proportion of hotspot area with combinations of vectors with suitability scores ≥ 0.5 . Fill colors represent unique vector combinations. BF, blackfly; BF-SF, black fly and sand fly; BM, biting midge; BM-SF, biting midge and sand fly; BM-BF, biting midge and black fly; BM-BF-SF, biting midge, blackfly, sand fly; SF, sand fly.

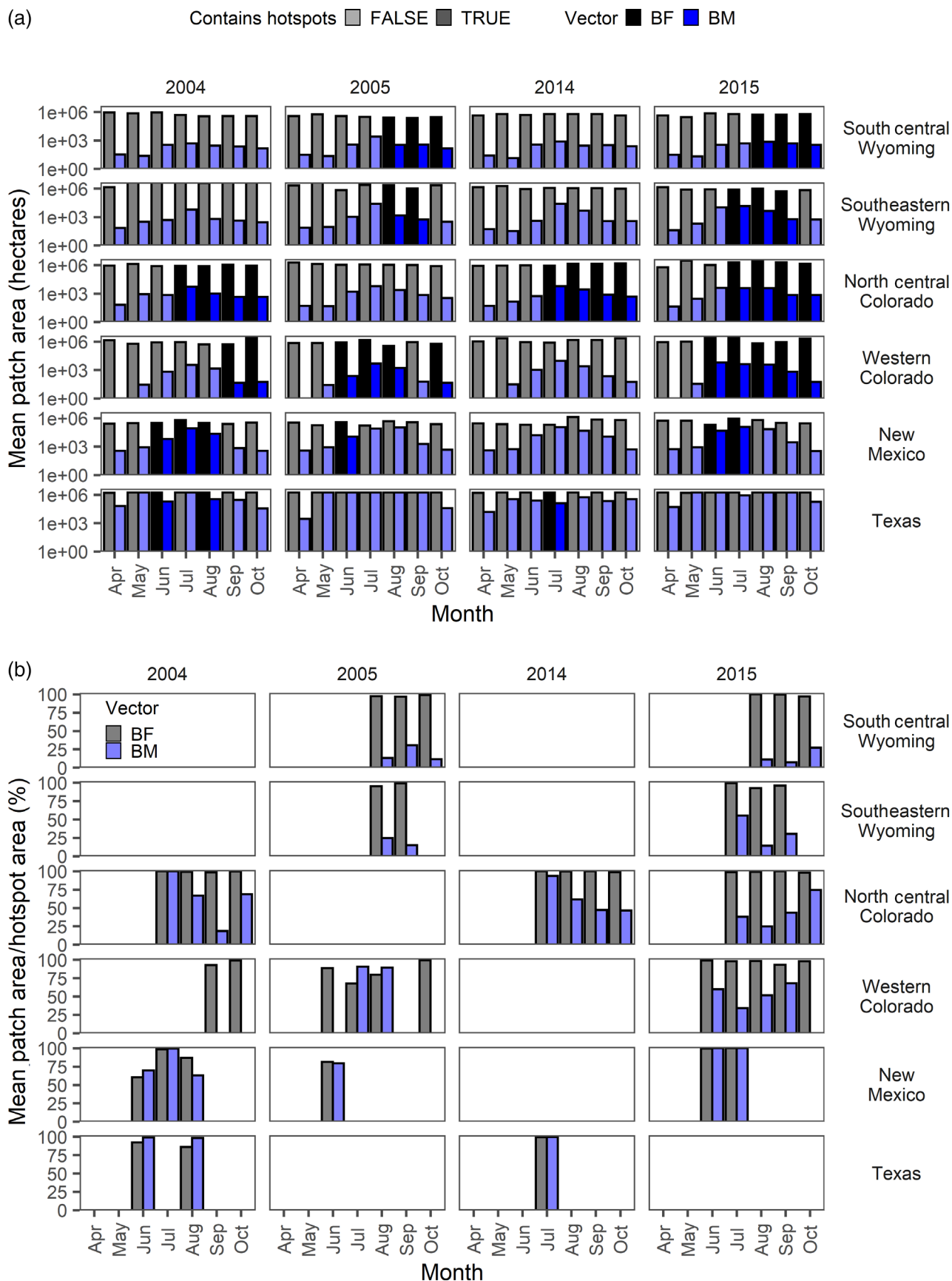


FIGURE 11 (a) The mean patch size of suitable habitat per vector per month. Fill colors represent unique vectors, though sand flies are omitted due to limited patch occurrence and area. Opacity represents whether the region of interest contains hotspots (dark) or not (light) during the month. (b) The mean patch size of suitable habitat within hotspots relative to hotspot area. BF, blackfly; BM, biting midge.

TABLE 3 Vector implication summary for each region of interest (ROI).

ROI	Vector	Implication
SC-WY	BM	Majority of irrigation by surface flooding (Appendix S1: Figure S2)
	BF	High perennial stream density (Appendix S1: Figure S1)
		Region >90% area with close proximity to flowing water (Figure 3)
		Hotspots have greater area near flowing water (Figure 6)
		Disproportionate LULC under hotspots for cultivated crops, i.e., nutrient input source for flowing water (Figure 7)
		Greater area suitable in region (Figure 10a) and hotspots (Figure 10b)
		Highest median suitability scores in hotspots (Figure 9)
SE-WY	BM	Majority of irrigation by surface flooding and high proportion of area flooded (Appendix S1: Figure S2)
	BF	High perennial stream and canal density (Appendix S1: Figure S1)
		Region >80% area with close proximity to flowing water and >75% area with close proximity to nutrient-rich flowing water, which is less than some ROI (Figure 3)
		Hotspots have greater area near flowing water (Figure 6)
		Consistently ~75% suitable area in region (Figure 10a), and >80% suitable area in hotspots (Figure 10b)
		Consistently large habitat patch size in regions (Figure 11a), consuming whole hotspots (Figure 11b)
	SF	High dry drainage cover
NC-CO	BM	About half irrigation by surface flooding and high proportion of area flooded (Appendix S1: Figure S2)
	BF	Hotspot timing coincides with elevated suitability in region (Figure 10a)
		High perennial stream and canal density (Appendix S1: Figure S1)
		Region >90% area with close proximity to flowing water and >85% area with close proximity to nutrient-rich flowing water (Figure 3)
		Hotspots have greater area near flowing water (Figure 6)
		Disproportionate LULC under hotspots for cultivated crops and urban areas, i.e., nutrient input source for flowing water (Figure 7)
		Highest median suitability scores in hotspots (Figure 9)
W-CO	BM	Majority of irrigation by surface flooding and high proportion of area flooded (Appendix S1: Figure S2)
	BF	Consistently ~80% suitable area in region (Figure 10a), but >95% suitable area in hotspots (Figure 10b)
		Consistently large habitat patch size in regions (Figure 11a), consuming whole hotspots (Figure 11b)
		High dry drainage cover
		High perennial stream and canal density (Appendix S1: Figure S1)
		Region >90% area with close proximity to flowing water and >80% area with close proximity to nutrient-rich flowing water (Figure 3)
		Hotspots have greater area near flowing water (Figure 6)
NM	BM	Disproportionate LULC under hotspots for cultivated crops and urban areas, i.e., nutrient input source for flowing water (Figure 7)
	BF	Highest median suitability scores in hotspots (Figure 9)
		Consistently ~75% suitable area in region (Figure 10a), and >80% suitable area in hotspots (Figure 10b)
		Consistently large habitat patch size in regions (Figure 11a), consuming >50% of hotspot area (Figure 11b)
		High dry drainage cover
		High percent dry area
	SF	High dry drainage cover

(Continues)

TABLE 3 (Continued)

ROI	Vector	Implication
TX	BM	Region >30% area with close proximity to wetted ground (Figure 3)
		Region: higher NDVI (Figure 3)
		Hotspots: high NDVI and more proximity to wetted ground than flowing water in 2014 (Figure 6)
		Preference for wetlands in 2014 (Figure 7)
		High suitability in region and hotspots (Figure 10a,b)
	BF	Consistently large habitat patch size in regions (Figure 11a), consuming whole hotspots (Figure 11b)
		Region >90% area with close proximity to flowing water and >90% area with close proximity to nutrient-rich flowing water (Figure 3)
		Highest median suitability scores in hotspots (Figure 9)
		Mostly ~95% suitable area in region (Figure 10a), and >95% suitable area in hotspots (Figure 10b)
SF	SF	Consistently large habitat patch size in regions, consuming whole hotspots (Figure 11b)
		High deciduous forest cover
		High temperature and vapor pressure (Figure 3)
		High temperature and vapor pressure in 2004 hotspots

Abbreviations: BF, black fly; BM, biting midge; LULC, Land Use Land Cover; NC-CO, north central Colorado; NDVI, normalized difference vegetation index; NM, New Mexico; SC-WY, south central Wyoming; SE-WY, southeastern Wyoming; SF, sand fly; TX, Texas; W-CO, western Colorado.

CONCLUSIONS

We selected six ROIs from the western US to investigate environmental conditions supportive of competent VS vectors. Summarized conditions associated with each vector by ROI provided a data-driven, spatial approach for this weight of evidence analysis (Table 3). Most evidence supported BF as the likely vector in northern ROI. Environmental conditions indicative of BM was the most consistent in TX and NM, but varied by ROI and over time. SF habitat was rare.

This paper focused on the known VS disease vector species of BF (*S. vittatum* complex), BM (*BM Culicoides variipennis* complex, which includes *C. sonorensis*), and SF (*L. shannoni*), the three species of biting flies most incriminated as transmission vectors for VSV. More research is needed to determine whether additional vectors are important, as they likely have different habitats, host preferences, dispersal, and behaviors. Some species may only be vectors during warmer and humid environmental conditions, when some insects may have increased longevity and potentially reduced extrinsic viral incubation periods. Shorter extrinsic incubation periods were observed for BM and blue tongue virus (Carpenter et al., 2011; Mullens et al., 1995), but the incubation periods for BM and VSV have not yet been tested. Conversely, most larval stages gain more mass under colder temperatures; therefore, cool and wet conditions may result in prolonged larval stages, leading to larger, longer-lived adults. How insect mass affects dispersal ability and distance is unknown. To account for this uncertainty, habitat descriptions and dispersal estimates for each vector insect family was intentionally broad to cover possible unknown vector species and limitations in

our current knowledge. As more vector and VS outbreak data become available, this novel approach can be applied to other locations and for other vector species to better understand the complex environment, host, vector, and pathogen relationship.

Peters et al. (2018) found that environmental conditions were primarily associated with BF habitat in incursion years, and both BF and BM habitat in expansion years. They considered the entire spatial extent of VS occurrences from 2004 to 2015, and did not consider regional variability, which is the focus of this paper. A second analysis investigated within-year variability in important VS vectors to come up with a sequence of important environmental conditions occurring within each type of year (incursion vs. expansion). This study corroborates those findings in that host density and environmental variables were important in explaining VS occurrence.

Elias et al. (2019) found that VS incidents were distributed near lotic habitat. Monthly incidents were closest to lotic habitat in April and furthest from lotic habitat in winter, indicating that initial infection near streams may spread away from these locations. This analysis found hotspots closer to flowing water and in ROI with higher stream and canal density and irrigation. Vector suitability scores for each ROI and hotspot varied through the year, but often suitable habitat for both BF and BM occurred later in the season in CO and WY watersheds, consistent with hotspots and with potential expansion of infected animals beyond the stream network.

Enhanced knowledge about VS vectors via field and laboratory studies will fill key knowledge gaps. Investigating the role of vectors, including potential dispersion distances, and potential wild animal hosts would

deepen our understanding of VS. Future work to compare habitat suitability with vector sampling data and explicitly include genetic data will deepen our knowledge about vector–habitat relationship in VS occurrence in both incursion and expansion years. Ultimately, supplementing early warning strategies (Peters et al., 2020) for this disease and other vector-borne diseases with regional context of vector suitability will help target protective actions to limit VS spread. This habitat analysis indicates BF habitat is the most consistent across all ROIs, but variable BM habitat is important in some ROI during some times of the year and SF habitat appears limited in most ROI. Given limited existing vector data, this analysis provides an alternate means to estimate likely vectors responsible for transmission. In addition, we recommend both serosurveillance in livestock and VSV surveillance in vectors (BF, BM, and SF) between VS outbreaks to provide baseline information for comparison when future outbreaks occur. The results could support early warning and mitigation efforts to reduce incidences of VS.

ACKNOWLEDGMENT

This research used resources provided by the SCINet project of the USDA Agricultural Research Service, ARS project number 0500-00093-001-00-D.

CONFLICT OF INTEREST


The authors declare no conflict of interest.

DATA AVAILABILITY STATEMENT

Datasets utilized for this research are as follows: USDA NASS (2017), Dewitz (2019), USGS (2020a), USGS (2020b), Dieter et al. (2018), Soil Survey Staff (2020), Didan (2015), JRC (2020), and Thornton et al. (2018). Vesicular stomatitis virus (VSV) location data at the scale used here are sensitive and cannot be provided publicly. The same VSV data summarized at the county level are publicly available from the United States Department of Agriculture Animal and Plant Health Inspection Service (USDA-APHIS) under the situation reports listed here: <https://www.aphis.usda.gov/aphis/ourfocus/animalhealth/animal-disease-information/cattle-disease-information/vesicular-stomatitis-info>. Finer-scale VSV data supporting this research are available from the USDA-APHIS-Veterinary Services, with restrictions, and are not accessible to the public. Please contact equine.health@usda.gov for VS data inquiries.

ORCID

Emile Elias  <https://orcid.org/0000-0001-9964-3177>

Heather M. Savoy  <https://orcid.org/0000-0002-2032-4868>

Debra P. C. Peters  <https://orcid.org/0000-0002-5842-8099>

REFERENCES

- Adler, P. H., D. C. Currie, and D. M. Wood. 2004. *The Black Flies (Simuliidae) of North America* 941. Ithaca, NY: Cornell University Press.
- Adler, P. H., and K. C. Kim. 1984. “Ecological Characterization of Two Sibling Species, IHL-1 and IS-7, in the *Simulium vittatum* Complex (Diptera: Simuliidae).” *Canadian Journal of Zoology* 62: 1308–15.
- Al-Kindi, K. M., P. Kwan, N. R. Andrew, and M. Welch. 2017. “Modelling Spatiotemporal Patterns of Dubas Bug Infestations on Date Palms in Northern Oman: A Geographical Information System Case Study.” *Crop Protection* 93: 113–21. <https://doi.org/10.1007/s10530-014-0802-2>.
- Baldwin, W. F., A. S. West, and J. Gomery. 1975. “Dispersal Pattern of Black Flies (Diptera: Simuliidae) Tagged with ^{32}P .” *Canadian Entomologist* 107: 113–8.
- Baylis, M., H. Bouayoune, J. Touti, and H. El Hasnaoui. 1998. “Use of Climatic Data and Satellite Imagery to Model the Abundance of *Culicoides Imicola*, the Vector of African Horse Sickness Virus, in Morocco.” *Medical and Veterinary Entomology* 12(3): 255–66. <https://doi.org/10.1046/j.1365-2915.1998.00109.x>.
- Bennet, G. F. 1963. “Use of P^{32} in the Study of a Population of *Simulium rugglesi* (Diptera: Simuliidae) in Algonquin Park, Ontario.” *Canadian Journal of Zoology* 41: 947–62.
- Bivand, R. S., E. Pebesma, and V. Gomez-Rubio. 2013. *Applied Spatial Data Analysis with R*, 2nd ed. NY: Springer.
- Buck, A. L. 1981. “New Equations for Computing Vapor Pressure and Enhancement Factor.” *Journal of Applied Meteorology* 20: 1527–32.
- Burgin, L. E., J. Gloster, C. Sanders, P. S. Mellor, S. Gubbins, and S. Carpenter. 2013. “Investigating Incursions of Bluetongue Virus Using a Model of Long-Distance *Culicoides* Biting Midge Dispersal.” *Transboundary and Emerging Diseases* 60: 263–72. DOI: [10.1111/j.1865-1682.2012.01345.x](https://doi.org/10.1111/j.1865-1682.2012.01345.x)
- Carpenter, S., A. Wilson, J. Barber, E. Veronesi, P. Mellor, G. Venter, and S. Gubbins. 2011. “Temperature Dependence of the Extrinsic Incubation Period of Orbiviruses in *Culicoides* Biting Midges.” *PLoS One* 6(11): e27987. <https://doi.org/10.1371/journal.pone.0027987>.
- Claborn, D. M., E. D. Rowton, P. G. Lawyer, G. C. Brown, and L. W. Keep. 2009. “Species Diversity and Relative Abundance of Phlebotomine SFs (Diptera: Psychodidae) and Three Army Installations in the Southern United States and Susceptibility of a Domestic SF to Infection with Old World *Leishmania major*.” *Military Medicine* 174(11): 1203–8. <https://doi.org/10.7205/MILMED-D-00-4309>.
- Cohen, Y. R. Sharon, T. Sokolsky, and T. Zahavi. 2011. “Modified Hot-Spot Analysis for Spatio-Temporal Analysis: A Case Study of the Leaf-Roll Virus Expansion in Vineyards.” *Spatial 2-Spatial Data Methods for Environmental and Ecological Processes*, 2011 At: Foggia, Italy.
- Comer, J. A., R. B. Tesh, G. B. Modi, J. L. Corn, and V. F. Nettles. 1990. “Vesicular Stomatitis Virus, New Jersey Serotype: Replication and Transmission by *Lutzomyia shannoni* (Diptera: Psychodidae).” *The American Journal of Tropical*

- Medicine and Hygiene* 42(5): 483–90. <https://doi.org/10.4269/ajtmh.1990.42.483>.
- Dewitz, J. 2019. “National Land Cover Database (NLCD) 2016 Products (Version 2.0, July 2020): US Geological Survey Data Release.” <https://doi.org/10.5066/P96HHBIE>.
- Diarra, M., M. Fall, R. Lancelot, A. Diop, A. G. Fall, A. Dicko, M. T. Seck, et al. 2015. “Modelling the Abundances of Two Major *Culicoides* (Diptera: Ceratopogonidae) Species in the Niayes Area of Senegal.” *PLoS One* 10(6): e0131021. <https://doi.org/10.1371/journal.pone.0131021>.
- Didan, K. 2015. “MOD13Q1 MODIS/Terra Vegetation Indices 16-Day L3 Global 250 m SIN Grid V006 [Data Set].” NASA EOSDIS Land Processes DAAC. <https://doi.org/10.5067/MODIS/MOD13Q1.006>.
- Dieter, C. A., K. S. Linsey, R. R. Caldwell, M. A. Harris, T. I. Ivahnenko, J. K. Lovelace, M. A. Maupin, and N. L. Barber. 2018. “Estimated Use of Water in the United States County-Level Data for 2015 (Version 2.0, June 2018): US Geological Survey Data Release.” <https://doi.org/10.5066/F7TB15V5>.
- Drolet, B. S., C. L. Campbell, M. A. Stuart, and W. C. Wilson. 2005. “Vector Competence of *Culicoides sonorensis* (Diptera: Ceratopogonidae) for Vesicular Stomatitis Virus.” *Journal of Medical Entomology* 42(3): 409–18. [https://doi.org/10.1603/0022-2585\(2005\)042\[0409:vcocsd\]2.0.co;2](https://doi.org/10.1603/0022-2585(2005)042[0409:vcocsd]2.0.co;2). PMID: 15962795.
- Duarte, P. C., P. S. Morley, J. L. Traub-Dargatz, and L. H. Creekmore. 2008. “Factors Associated with Vesicular Stomatitis in Animals in the Western United States.” *Journal of the American Veterinary Medical Association* 232: 249–56.
- Elias, E., D. S. McVey, D. Peters, J. D. Derner, A. Pelzel-McCluskey, T. S. Schrader, and L. Rodriguez. 2019. “Contributions of Hydrology to Vesicular Stomatitis Virus Emergence in the Western USA.” *Ecosystems* 22: 416–33.
- Fei, S. 2010. “Applying Hotspot Detection Methods in Forestry: A Case Study of Chestnut Oak Regeneration.” *International Journal of Forestry Research* 2010: 1–8.
- Ferro, C., E. Cárdenas, D. Corredor, A. Morales, and L. E. Munstermann. 1998. “Life Cycle and Fecundity Analysis of *Lutzomyia shannoni* (Dyar) (Diptera: Psychodidae).” *Memórias do Instituto Oswaldo Cruz* 93(2): 195–9.
- Fredeen, F. J. H. 1969. “Outbreaks of the Black Fly *Simulium arcticum* Malloch in Alberta.” *Quaestiones Entomologicae* 5: 341–72.
- GDAL/OGR Contributors. 2020. “GDAL/OGR Geospatial Data Abstraction Software Library.” Open Source Geospatial Foundation. <https://gdal.org>.
- Gergely K. J., K. G. Boykin, A. J. McKerrow, M. J. Rubino, N. M. Tarr, and S. G. Williams. 2019. “Gap Analysis Project (GAP) Terrestrial Vertebrate Species Richness Maps for the Conterminous US: US Geological Survey Scientific Investigations Report 2019–5034.” 99 p. <https://doi.org/10.3133/sir20195034>.
- Getis, A., and J. Aldstadt. 2004. “Constructing the Spatial Weights Matrix Using a Local Statistic.” *Geographical Analysis* 36: 90–104.
- Getis, A., A. C. Morrison, K. Gray, and T. W. Scott. 2010. “Characteristics of the Spatial Pattern of the Dengue Vector, *Aedes aegypti*, in Iquitos, Peru.” In *Perspectives on Spatial Data Analysis. Advances in Spatial Science (The Regional Science Series)*, edited by L. Anselin and S. Rey. Berlin, Heidelberg: Springer.
- Getis, A., and J. K. Ord. 1992. “The Analysis of Spatial Association by Use of Distance Statistics.” *Geographical Analysis* 24: 189–206.
- Gislason, G. M., T. Hrafnisdóttir, and A. Gardarsson. 1994. “Long-Term Monitoring of Numbers of Chironomidae and Simuliidae in the River Laxá, North Iceland.” *Verhandlungen - Internationale Vereinigung für Theoretische und Angewandte Limnologie* 25: 1492–5.
- Gorelick, N., M. Hancher, M. Dixon, S. Ilyushchenko, D. Thau, and R. Moore. 2017. “Google Earth Engine: Planetary-Scale Geospatial Analysis for Everyone.” *Remote Sensing of Environment* 202: 18–27.
- Haddow, A. D., G. Curler, and J. K. Moulton. 2008. “New Records of *Lutzomyia shannoni* and *Lutzomyia vexator* (Diptera: Psychodidae) in Eastern Tennessee.” *Journal of Vector Ecology* 33(2): 393–6. DOI: [10.3376/1081-1710-33.2.393](https://doi.org/10.3376/1081-1710-33.2.393)
- Harris, N. L., E. Goldman, C. Gabris, J. Nordling, S. Minnemeyer, S. Ansari, M. Lippmann, et al. 2017. “Using Spatial Statistics to Identify Emerging Hot Spots of Forest Loss.” *Environmental Research Letters* 12: 024012.
- Hesselbarth, M. H. K., M. Sciaini, K. A. With, K. Wiegand, and J. Nowosad. 2019. “landscapemetrics: An Open-Source R Tool to Calculate Landscape Metrics.” *Ecography* 42: 1648–57.
- Homer, C. G., J. A. Dewitz, S. Jin, G. Xian, C. Costello, P. Danielson, L. Gass, et al. 2020. “Conterminous United States Land Cover Change Patterns 2001–2016 from the 2016 National Land Cover Database.” *ISPRS Journal of Photogrammetry and Remote Sensing* 162: 184–99.
- Hurd, H. S., B. J. McCluskey, and E. L. Mumford. 1999. “Management Factors Affecting the Risk for Vesicular Stomatitis in Livestock Operations in the Western United States.” *Journal of the American Veterinary Medical Association* 215(9): 1263–8.
- Joint Research Centre (JRC). 2020. “Global Surface Water – Data Access.” European Commission Joint Research Centre. <https://global-surface-water.appspot.com/download>.
- Killmaster, L. F., D. E. Stallknecht, E. W. Howerth, J. K. Moulton, P. F. Smith, and D. G. Mead. 2010. *Apparent Disappearance of Vesicular Stomatitis New Jersey Virus from Ossabaw Island, Georgia: Vector-Borne and Zoonotic Diseases*. <https://doi.org/10.1089/vbz.2010.0083>.
- Kracalik, I. T., J. K. Blackburn, L. Lukhnova, Y. Pazilov, M. E. Hugh Jones, and A. Aikimbayev. 2013. “Analyzing the Spatial Patterns of Livestock Anthrax in Kazakhstan in Relation to Environmental Factors: A Comparison of Local (G_i^*) and Morphology Cluster Statistics.” *Geospatial Health* 7: 111–26.
- Lambin, E. F., A. Tran, S. O. Vanwambeke, C. Linard, and V. Soti. 2010. “Pathogenic Landscapes: Interactions between Land, People, Disease Vectors, and their Animal Hosts.” *International Journal of Health Geographics* 9: 54. <https://doi.org/10.1186/1476-072X-9-54>.
- Lillie, T. W., W. C. Marquardt, and R. Jones. 1981. “The Flight Range of *Culicoides variipennis* (Diptera: Ceratopogonidae).” *The Canadian Entomologist* 113(5): 419–26.
- Mayo, C. E., C. J. Osborne, B. A. Mullens, A. C. Gerry, I. A. Gardner, W. K. Reisen, C. M. Barker, and N. J. MacLachlan.

2014. "Seasonal Variation and Impact of Waste-Water Lagoons as Larval Habitat on the Population Dynamics of *Culicoides sonorensis* (Diptera: Ceratopogonidae) at Two Dairy Farms in Northern California." *PLoS One* 9(2): e89633. <https://doi.org/10.1371/journal.pone.0089633>.
- McCluskey, B. J., B. J. Beaty, and M. D. Salman. 2003. "Climatic Factors and the Occurrence of Vesicular Stomatitis in New Mexico, United States of America." *Revue Scientifique et Technique* 22(3): 849–56.
- Mead, D. G., C. J. Mare, and E. W. Cupp. 1997. "Vector Competence of Select Black Fly Species for Vesicular Stomatitis Virus (New Jersey Serotype)." *The American Journal of Tropical Medicine and Hygiene* 57(1): 42–8. <https://doi.org/10.4269/ajtmh.1997.57.42>.
- Mead, D. G., C. J. Mare, and F. B. Ramberg. 1999. "Bite Transmission of Vesicular Stomatitis Virus (New Jersey Serotype) to Laboratory Mice by *Simulium vittatum* (Diptera: Simuliidae)." *Journal of Medical Entomology* 35(4): 410–3. DOI: [10.1093/jmedent/36.4.410](https://doi.org/10.1093/jmedent/36.4.410)
- Miller, R. S., S. J. Sweeney, C. Sloodmaker, D. A. Grear, P. A. Di Salvo, D. Kiser, and S. A. Shwiff. 2017. "Cross-Species Transmission Potential between Wild Pigs, Livestock, Poultry, Wildlife, and Humans: Implications for Disease Risk Management in North America." *Scientific Reports* 7: 7821. <https://doi.org/10.1038/s41598-017-07336-z>.
- Minter, L., B. Kovacic, D. M. Claborn, P. Lawyer, D. Florin, and G. C. Brown. 2009. "New State Records of *Lutzomyia shannoni* and *Lutzomyia vexator*." *Journal of Medical Entomology* 46(4): 965–8. DOI: [10.1603/033.046.0432](https://doi.org/10.1603/033.046.0432)
- Moore, H. S., and R. Noblet. 1974. "Flight Range of *Simulium slossonae*, the Primary Vector of *Leucocytozoon smithi* of Turkeys in South Carolina." *Environmental Entomology* 3: 365–9.
- Morin, A., and R. H. Peters. 1988. "Effect of Microhabitat Features, Seston Quality, and Periphyton on Abundance of Overwintering Black Fly Larvae in Southern Québec." *Limnology and Oceanography* 33: 431–46.
- Mullen, G. R., and C. S. Murphree. 2019. "Biting Midges (Ceratopogonidae)." In *GR Mullen and LA Durden, Medical and Veterinary Entomology*, 3rd ed. 213–36. Cambridge, MA: Academic Press. <https://doi.org/10.1016/B978-0-12-814043-7.00013-3>.
- Mullens, B. A., W. J. Tabachnick, F. R. Holbrook, and L. H. Thompson. 1995. "Effects of Temperature on Virogenesis of Bluetongue Virus Serotype 11 in *Culicoides variipennis* Sonorensis." *Medical and Veterinary Entomology* 9(1): 71–6. <https://doi.org/10.1111/J.1365-2915.1995.TB00119.X>.
- Munstermann, L. E. 2005. "Phlebotomine Sand Flies, the Psychodidae." In *Biology of Disease Vectors*, edited by W. C. Marquardt, 2nd ed. 141–51. Burlington, MA: Elsevier Academic Press.
- National Agricultural Statistics Service (NASS). 2017. "NASS – Quick Stats." USDA National Agricultural Statistics Service. <https://data.nal.usda.gov/dataset/nass-quick-stats>.
- Oliveira, A., L. W. Cohnstaedt, L. E. Noronha, D. Mitzel, D. S. McVey, and N. Cernicchiaro. 2020. "Perspectives Regarding the Risk of Introduction of the Japanese Encephalitis Virus (JEV) in the United States." *Frontiers in Veterinary Science* 7: 48. <https://doi.org/10.3389/fvets.2020.00048>.
- Ord, J. K., and A. Getis. 1995. "Local Spatial Autocorrelation Statistics: Distributional Issues and an Application." *Geographical Analysis* 27(4): 286–306.
- Palinski, R., S. J. Pauszek, J. M. Humphreys, D. P. C. Peters, D. S. McVey, A. M. Pelzel-McCluskey, J. D. Derner, N. D. Burruss, J. Arzt, and L. L. Rodriguez. 2021. "Evolution and Expansion Dynamics of a Vector-Borne Virus: 2004–2006 Vesicular Stomatitis Outbreak in the Western USA." *Ecosphere* 12(10): e03793. <https://doi.org/10.1002/ecs2.3793>.
- Peck, D. E., W. K. Reeves, A. M. Pelzel-McCluskey, J. D. Derner, B. Drolet, L. W. Cohnstaedt, D. Swanson, D. S. McVey, L. L. Rodriguez, and D. P. C. Peters. 2020. "Management Strategies for Reducing the Risk of Equine Contracting Vesicular Stomatitis Virus (VSV) in the Western United States." *Journal of Equine Veterinary Science* 90: 103026.
- Pekel, J. F., A. Cottam, N. Gorelick, and A. S. Belward. 2016. "High-Resolution Mapping of Global Surface Water and its Long-Term Changes." *Nature* 540(7633): 418–22. <https://doi.org/10.1038/nature20584>.
- Perez, A. M., S. J. Pauszek, D. Jimenez, W. N. Kelley, Z. Whedbee, and L. L. Rodriguez. 2010. "Spatial and Phylogenetic Analysis of Vesicular Stomatitis Virus over-Wintering in the United States." *Preventive Veterinary Medicine* 93(4): 258–64.
- Perez De Leon, A. A., D. O'Toole, and W. J. Tabachnick. 2006. "Infection of Guinea Pigs with Vesicular Stomatitis New Jersey Virus Transmitted by *Culicoides sonorensis* (Diptera: Ceratopogonidae)." *Journal of Medical Entomology* 43(3): 568–73.
- Perez de Leon, A. A., and W. J. Tabachnick. 2006. "Transmission of Vesicular Stomatitis New Jersey Virus to Cattle by the Biting Midge *Culicoides sonorensis* (Diptera: Ceratopogonidae)." *Journal of Medical Entomology* 43(2): 323–9.
- Peters, D. P. C., N. D. Burruss, L. L. Rodriguez, D. S. McVey, E. H. Elias, A. M. Pelzel-McCluskey, J. D. Derner, et al. 2018. "An Integrated View of Complex Landscapes: A Big Data-Model Integration Approach to Transdisciplinary Science." *Bioscience* 68(9): 653–69. <https://doi.org/10.1093/biosci/biy069>.
- Peters, D. P. C., D. S. McVey, E. H. Elias, A. M. Pelzel-McCluskey, J. D. Derner, N. D. Burruss, T. S. Schrader, et al. 2020. "Big Data-Model Integration and AI for Vector-Borne Disease Prediction." *Ecosphere* 11: e03157.
- Price, D. C., D. E. Gunther, and R. Gaugler. 2011. "First Collection Records of Phlebotomine Sand Flies (Diptera: Psychodidae) from New Jersey." *Journal of Medical Entomology* 48(2): 476–8. <https://doi.org/10.1603/ME10170>.
- R Core Team. 2020. *R: A Language and Environment for Statistical Computing*. Vienna: R Foundation for Statistical Computing. <https://www.R-project.org/>.
- Ready, P. D. 2013. "Biology of Phlebotomine Sand Flies as Vectors of Disease Agents." *Annual Review of Entomology* 58: 227–50.
- Reisen, W. K. 2010. "Landscape Epidemiology of Vector-Borne Diseases." *Annual Review of Entomology* 55(1): 461–83. DOI: [10.1146/annurev-ento-112408-085419](https://doi.org/10.1146/annurev-ento-112408-085419)
- Rodriguez, L., T. A. Bunch, M. Fraire, and Z. N. Llewellyn. 2000. "Re-Emergence of Vesicular Stomatitis in the Western United States is Associated with Distinct Viral Genetic Lineages." *Virology* 271(1): 171–81.
- Rodríguez, L. L. 2002. "Emergence and Re-Emergence of Vesicular Stomatitis in the United States." *Virus Research* 85: 211–9.

- Rozo-Lopez, P., B. S. Drolet, and B. Londoño-Rentería. 2018. "Vesicular Stomatitis Virus Transmission: A Comparison of Incriminated Vectors." *Insects* 9: 190. <https://doi.org/10.3390/insects9040190>.
- Sellers, R., and A. Maarouf. 1990. "Trajectory Analysis of Winds and Vesicular Stomatitis in North America, 1982–5." *Epidemiology and Infection* 104(2): 313–28. <https://doi.org/10.1017/S0950268800059495>.
- Soil Survey Staff. 2020. "Gridded National Soil Survey Geographic (gNATSGO) Database for the Conterminous United States. United States Department of Agriculture, Natural Resources Conservation Service." <https://nrcs.app.box.com/v/soils>. (FY2020 official release).
- Stone, A., and E. L. Snoddy. 1969. "The Black Flies of Alabama (Diptera: Simuliidae)." *Auburn University Agricultural Experiment Bulletin* 390: 1–93.
- Sumaye, R. D., E. Geubbels, E. Mbeyela, and D. Berkvens. 2013. "Inter-Epidemic Transmission of Rift Valley Fever in Livestock in the Kilombero River Valley, Tanzania: A Cross-Sectional Survey." *PLoS Neglected Tropical Diseases* 7: e2356.
- Thornton, P. E., M. M. Thornton, B. W. Mayer, Y. Wei, R. Devarakonda, R. S. Vose, and R. B. Cook. 2018. *Daymet: Daily Surface Weather Data on a 1-km Grid for North America, Version 3*. Oak Ridge, TN: ORNL DAAC. <https://doi.org/10.3334/ORNLDAAAC/1328>.
- United States Department of Agriculture (USDA). 2020. "Vesicular Stomatitis." <https://www.aphis.usda.gov/aphis/ourfocus/animalhealth/animal-disease-information/cattle-disease-information/vesicular-stomatitis-info>.
- United States Geological Survey (USGS). 2020a. National Geospatial Program, 20200827. "USGS National Hydrography in FileGDB 10.1 format (published 20200827) Model Version 2.2.1." US Geological Survey. <https://www.sciencebase.gov/catalog/item/5ea068ae82cefae35a12a120>.
- United States Geological Survey (USGS). 2020b. "USGS National Watershed Boundary Dataset in FileGDB 10.1 Format (Published 20201002)." US Geological Survey. <https://www.sciencebase.gov/catalog/item/61fd7d49d34e622189cf3aab>.
- Venables, W. N., and B. D. Ripley. 2002. *Modern Applied Statistics with S*, 4th ed. New York: Springer.
- Walsh, M. G., and C. Webb. 2018. "Hydrological Features and the Ecological Niches of Mammalian Hosts Delineate Elevated Risk for Ross River Virus Epidemics in Anthropogenic Landscapes in Australia." *Parasites and Vectors* 11(1): 1–11. <https://doi.org/10.1186/s13071-018-2776-x>.
- Weng, J.-L., S. L. Young, D. M. Gordon, D. Claborn, C. Peterson, and M. Ramalho-Ortigao. 2012. "First Report of Phlebotomine Sand Flies (Diptera: Psychodidae) in Kansas and Missouri, and a PCR Method to Distinguish *Lutzomyia shannoni* from *Lutzomyia vexator*." *Journal of Medical Entomology* 49(6): 1460–5.
- Young, D. G., and M. A. Duncan. 1994. *Guide to the Identification and Geographic Distribution of Lutzomyia Sand Flies in Mexico, the West Indies, Central and South America (Diptera: Psychodidae)* 881. Gainesville, FL: Assoc Publ Mem Am Entomol Inst.
- Young, D. G., and P. V. Perkins. 1984. "Phlebotomine Sand Flies of North America (Diptera: Psychodidae)." *Mosquito News* 44(2): 263–304.

SUPPORTING INFORMATION

Additional supporting information can be found online in the Supporting Information section at the end of this article.

How to cite this article: Elias, Emile, Heather M. Savoy, Dustin A. Swanson, Lee W. Cohnstaedt, Debra P. C. Peters, Justin D. Derner, Angela Pelzel-McCluskey, Barbara Drolet, and Luis Rodriguez. 2022. "Landscape Dynamics of a Vector-Borne Disease in the Western US: How Vector-Habitat Relationships Inform Disease Hotspots." *Ecosphere* 13(11): e4267. <https://doi.org/10.1002/ecs2.4267>